



Low dose Btk inhibitors selectively block platelet activation by CLEC-2

by Phillip L.R. Nicolson, Sophie H. Nock, Joshua Hinds, Lourdes Garcia-Quintanilla, Christopher W. Smith, Joana Campos, Alexander Brill, Jeremy A. Pike, Abdullah O. Khan, Natalie S. Poulter, Diedre M. Kavanagh, Stephanie Watson, Callum N. Watson, Hayley Clifford, Aarnoud P. Huissoon, Alice Y. Pollitt, Johannes A. Eble, Guy Pratt, Steve P. Watson, and Craig E. Hughes

Haematologica 2020 [Epub ahead of print]

*Citation: Phillip L.R. Nicolson, Sophie H. Nock, Joshua Hinds, Lourdes Garcia-Quintanilla, Christopher W. Smith, Joana Campos, Alexander Brill, Jeremy A. Pike, Abdullah O. Khan, Natalie S. Poulter, Diedre M. Kavanagh, Stephanie Watson, Callum N. Watson, Hayley Clifford, Aarnoud P. Huissoon, Alice Y. Pollitt, Johannes A. Eble, Guy Pratt, Steve P. Watson, and Craig E. Hughes. Low dose Btk inhibitors selectively block platelet activation by CLEC-2 Haematologica. 2020; 105:xxx
doi:10.3324/haematol.2019.218545*

Publisher's Disclaimer.

E-publishing ahead of print is increasingly important for the rapid dissemination of science. Haematologica is, therefore, E-publishing PDF files of an early version of manuscripts that have completed a regular peer review and have been accepted for publication. E-publishing of this PDF file has been approved by the authors. After having E-published Ahead of Print, manuscripts will then undergo technical and English editing, typesetting, proof correction and be presented for the authors' final approval; the final version of the manuscript will then appear in print on a regular issue of the journal. All legal disclaimers that apply to the journal also pertain to this production process.

Low dose Btk inhibitors selectively block platelet activation by CLEC-2

Names of Authors

Phillip LR Nicolson^{1,2}, Sophie H Nock³, Joshua Hinds¹, Lourdes Garcia-Quintanilla¹, Christopher W Smith¹, Joana Campos¹, Alexander Brill^{1,4}, Jeremy A Pike^{1,5}, Abdullah O Khan¹, Natalie S Poulter^{1,5}, Deidre M Kavanagh^{1,5}, Stephanie Watson¹, Callum N Watson¹, Hayley Clifford⁶, Aarnoud P Huissoon⁶, Alice Y Pollitt³, Johannes A Eble⁷, Guy Pratt², Steve P. Watson^{1,5} and Craig E Hughes³

Authors' Affiliations

¹Institute of Cardiovascular Sciences, College of Medical and Dental Sciences, University of Birmingham, UK

²Department of Haematology, Queen Elizabeth Hospital, Birmingham, UK

³Institute for Cardiovascular and Metabolic Research, Harborne Building, University of Reading, UK

⁴Department of Pathophysiology, Sechenov First Moscow State Medical University (Sechenov University), Moscow, Russia

⁵Centre of Membrane Proteins and Receptors (COMPARE), Universities of Birmingham and Nottingham, Midlands, UK

⁶Department of Immunology, Heartlands Hospital, Birmingham, UK

⁷Institute for Physiological Chemistry and Pathobiochemistry, University of Münster, Münster, Germany

Running head

Btk in CLEC-2-mediated platelet function and signalling

Contact information for correspondence

Dr Phillip LR Nicolson (p.nicolson@bham.ac.uk)

Prof Steve P Watson (s.p.watson@bham.ac.uk)

Dr Craig E Hughes (c.e.hughes@reading.ac.uk)

Word count (max 4000 words)

3191

Acknowledgements

This work was supported by British Heart Foundation (BHF) Programme grant (RG/13/18/30563), a BHF Clinical Fellowship to PLRN (FS/17/20/32738), a BHF Senior Basic Science Research Fellowship to AB (FS/19/30/34173), an AMS springboard grant to AYP (SBF002\1099) and the University of Birmingham's Institute of Translation Medicine and Institute of Cardiovascular Sciences; SPW holds a BHF Chair (CH03/003). JAE is supported by the Deutsche Forschungsgemeinschaft (DFG grant: Eb177/13-1).

Abstract (max 250 words)

Inhibitors of the tyrosine kinase Btk have been proposed as novel antiplatelet agents. In this study we show that low concentrations of the Btk inhibitor ibrutinib block CLEC-2-mediated activation and tyrosine phosphorylation including Syk and PLC γ 2 in human platelets. Activation is also blocked in patients with X-linked agammaglobulinaemia (XLA) caused by a deficiency or absence of Btk. In contrast, the response to GPVI is delayed in the presence of low concentrations of ibrutinib or in patients with XLA, and tyrosine phosphorylation of Syk is preserved. A similar set of results is seen with the second-

generation inhibitor, acalabrutinib. The differential effect of Btk inhibition in CLEC-2 relative to GPVI signalling is explained by the positive feedback role involving Btk itself, as well as ADP and thromboxane A₂ mediated activation of P2Y₁₂ and TP receptors, respectively. This feedback role is not seen in mouse platelets and, consistent with this, CLEC-2-mediated activation is blocked by high but not by low concentrations of ibrutinib. Nevertheless, thrombosis was absent in 8 out of 13 mice treated with ibrutinib. These results show that Btk inhibitors selectively block activation of human platelets by CLEC-2 relative to GPVI suggesting that they can be used at 'low dose' in patients to target CLEC-2 in thrombo-inflammatory disease.

Introduction

The C-type lectin receptor CLEC-2 is expressed at high levels on platelets and at low levels on a sub-population of haematopoietic cells¹. Its only known physiological ligand is podoplanin². Recent reports have demonstrated a critical role for CLEC-2 in inflammation-driven venous thrombosis^{3,4}, generating interest in drugs that target CLEC-2 in thrombo-inflammatory disorders whilst preserving haemostasis. This is further fuelled by the demonstration that CLEC-2 plays a minimal or negligible role in haemostasis (for review see Rayes *et al*⁵).

CLEC-2 has a cytoplasmic tail containing a single tyrosine in a conserved YxxL sequence in a motif that represents half of an immunoreceptor tyrosine-based activation motif (ITAM), known as a hemITAM. The conserved tyrosine is phosphorylated by the tyrosine kinase Syk⁶. This leads to recruitment of Syk through binding of its tandem SH2 domains and initiation of a downstream signalling cascade involving Src, Syk and Tec (including Btk) kinases, various adapter proteins including LAT, Gads, Grb-2 and SLP-76, the Vav family GTP exchange proteins and the effector protein, PLCγ2⁷⁻⁹. This hemITAM signalling pathway is similar to that used by the YxxL-containing platelet ITAM receptors such as the collagen receptor GPVI-FcγR complex and the low affinity immune receptor FcγRIIA¹⁰. A fundamental difference in these pathways however is that Syk binds to two phosphorylated tyrosines within a single ITAM in GPVI-FcγR and FcγRIIA, and to two phosphorylated hemITAMs in separate cytosolic receptor chains of CLEC-2¹¹. A further difference between CLEC-2 and GPVI signalling in human platelets is the critical dependence of CLEC-2 on positive feedback signalling through ADP and thromboxane A₂ (TxA₂), actin polymerisation, and the small GTPase Rac⁸. In contrast these positive feedback pathways play a relatively minor role in CLEC-2 signalling in mouse platelets¹².

Recently, irreversible inhibitors of the Tec kinase Btk have entered clinical use for the treatment of B-cell malignancies^{13,14}. These include the first-generation inhibitor ibrutinib and the second-generation inhibitor acalabrutinib. Ibrutinib is associated with a significant increase in major bleeding which is much reduced with the second generation inhibitor acalabrutinib^{14,15}. Patients with X-linked agammaglobulinaemia (XLA) who have function-disrupting mutations or loss of Btk however do not have increased bleeding. This observation, coupled with protein biochemistry measurements, have led us to conclude that the bleeding induced by ibrutinib is due to the high dosing strategy and off-target effects¹⁶. Platelets express two members of the Tec family of tyrosine kinases, namely Btk and Tec. Btk has an approximate 10-20 fold greater level of expression in both human and mouse platelets^{17,18}. Various studies have shown redundancy between the two kinases downstream of GPVI, with Tec able to partially compensate for the absence of Btk in human platelets from patients with XLA and in mouse platelets which are deficient in Btk^{16,19,20}.

Recently, Btk inhibitors have been proposed to represent a new class of anti-thrombotic drug (reviewed by Busygina *et al*²¹.) based on the observation that they delay or inhibit *ex vivo* platelet activation by GPVI^{16,22-24} and by immobilised atherosclerotic plaque at arterial rates of flow²⁵. In addition, Btk inhibitors block platelet activation by CLEC-2. However, in

contrast to GPVI, Manne *et al.* have proposed that Btk lies upstream of Syk in the CLEC-2 signalling cascade based on studies using ibrutinib-treated human platelets²⁶.

In the present study, we demonstrate that the results of Manne *et al.* are explained by the positive feedback role of ADP and TxA₂ and that concentrations of ibrutinib that have little or no effect on the response to GPVI stimulation selectively block activation by CLEC-2. This observation, together with the pivotal role of CLEC-2 in thrombo-inflammation, suggests that inhibitors of Btk represent new antiplatelet agents for thrombo-inflammatory disorders with minimal effect on haemostasis.

Methods

Platelet preparation

Blood was taken from consenting patients or healthy, drug-free volunteers, into 4% sodium citrate as previously described¹⁶. Mouse blood was drawn from CO₂ asphyxiated mice following isoflurane anaesthesia by inferior vena cava (IVC) puncture and taken into acid citrate dextrose (ACD). Platelet rich plasma (PRP) was obtained by centrifugation. Washed human and mouse platelets were obtained by further centrifugation of PRP in the presence of prostacyclin and resuspended in modified Tyrode's buffer as previously described¹⁶. Platelets were used at a cell density of 4x10⁸/ml for aggregometry and biochemical studies.

Light transmission aggregometry (LTA)

Aggregation was monitored by light transmission using a Model 700 aggregometer (Chronolog, Havertown, PA, USA) as previously described¹⁶.

Protein phosphorylation

Eptifibatide treated washed platelets were stimulated in a Model 700 aggregometer in the presence of ibrutinib or vehicle as described¹⁶. Activation was terminated after 300 seconds by addition of reducing sample buffer. This was followed by lysate separation by SDS-PAGE, electro-transfer and western blot as described previously¹⁶.

IVC stenosis assay

All mouse experiments were performed using wild type (WT) mice on a C57Bl/6 genetic background under Home Office project licences P0E98D513 and PC427E5DD. Mice were sourced from Charles River UK Ltd. (Margate, UK). For *ex vivo* platelet function assays and *in vivo* thrombosis assays 8 week old C57Bl/6 WT male mice were treated by intraperitoneal (IP) injection with a total dose of 140 mg/kg of ibrutinib or vehicle (5% DMSO, 30% Polyethylene glycol 300, 5% Tween 20, 60% deionised water) in divided doses once daily over 2 – 4 days. Blood was taken at the stated times and platelet function analysis was performed as described above using flow cytometry.

The IVC stenosis model was performed as described by Payne *et al*³. In brief, mice were anaesthetised using isoflurane and then a laparotomy was performed. Side branches of the IVC were identified and tied off before the IVC itself was stenosed with a ligature and a 30-gauge spacer to maintain a small degree of vessel patency. The incision was then closed and mice were allowed to recover from surgery. Buprenorphine was used pre- and post-operatively for analgesia. Mice were then culled 48 hours after the surgery and the IVC was examined for the presence and size of thrombus.

Other methods

Details of reagents and methods used for flow cytometry, flow adhesion, imaging, image analysis and cell transfection are detailed in the supplementary material.

Statistical analysis

All data are presented as mean \pm standard error of the mean with statistical significance taken as $p < 0.05$ unless otherwise stated. Statistical analysis was performed using Mann-Whitney tests, Fisher's exact test, Welch's t-test or one or two-way ANOVA with corrections for multiple comparisons as stated. Statistical analysis of the IC_{50} values was performed using Welch's t-test. All statistical analyses were performed using GraphPad Prism 7 (GraphPad Software Inc. La Jolla, Ca).

Ethical Approval

Ethical approval for collecting blood from patients and healthy volunteers was granted by the National Research Ethics Service (10/H1206/58) and Birmingham University Internal Ethical Review (ERN_11-0175) respectively. Work on patients with XLA has ethical approval via the University of Birmingham Human Biomaterials Resource Centre (16-251 Amendment 3).

Results

CLEC-2-mediated human platelet aggregation is inhibited by low concentrations of Btk inhibitors

To examine the role of Btk downstream of platelet CLEC-2 in humans we took healthy donor washed platelets and added increasing concentrations of ibrutinib before stimulating with the CLEC-2 agonist rhodocytin. As shown in Figure 1A-B, ibrutinib completely inhibited CLEC-2-mediated aggregation at concentrations as low as 70 nM. Inhibition was marked after 5 min incubation with ibrutinib and only increased slightly with times up to 60 min (Figure 1A-B and Supplementary Figure 1). Strikingly, the IC_{50} for inhibition was over 20-fold lower than that required to block GPVI-mediated platelet aggregation¹⁶ (Table 1). This selective inhibition of the response to CLEC-2 activation is consistent with the results of Manne *et al*²⁶.

We further studied the effect of *in vivo* Btk inhibition on PRP obtained from patients with chronic lymphocytic leukaemia (CLL) treated with ibrutinib or the more specific second generation Btk inhibitor acalabrutinib. Unlike platelets from patients treated with a control chemotherapy regimen (fludarabine, cyclophosphamide and rituximab; FCR), Btk inhibitor treated patients did not aggregate to even high levels of CLEC-2 stimulation (Figure 1C). We have previously shown that PRP from Btk inhibitor-treated patients do, however, aggregate to GPVI and G protein-coupled receptor (GPCR) stimulation¹⁶.

Adhesion to podoplanin under venous flow conditions is abrogated by Btk inhibition

Given the role of platelet CLEC-2 and podoplanin in the thrombo-inflammatory and venous thrombosis models performed by Hitchcock *et al*⁴ and Payne *et al*³ we investigated whether inhibition of CLEC-2-mediated platelet function by ibrutinib reduced or prevented adhesion to the endogenous ligand under flow. Blood from healthy donors, patients with XLA or those taking ibrutinib or acalabrutinib was flowed over podoplanin at venous shear. Strikingly we found that both platelet adhesion and platelet aggregate size were markedly reduced when compared to healthy donor blood regardless of the method of Btk inhibition (Figure 2).

Btk and Syk inhibition block CLEC-2-mediated Btk phosphorylation

To examine the effect of ibrutinib on CLEC-2-mediated protein phosphorylation, ibrutinib-treated washed human platelets were lysed after stimulation with rhodocytin and lysates probed with phosphospecific antibodies. As shown in Figure 3A, phosphorylation of Syk Y525/6, SLP-76 Y145, LAT Y200, Btk Y223 and Y551, and PLC γ 2 Y1217 was blocked by 70 nM ibrutinib with IC_{50} s similar to those for aggregation (Table 1). This concentration of

ibrutinib reduced total phosphotyrosine to basal levels and inhibited phosphorylation on all measured tyrosine sites except the constitutive phosphorylation of Src Y418. Loss of Src pY418 was seen at higher concentrations of ibrutinib (Figure 3Aiv) similar to our previous study¹⁶.

We performed similar experiments with acalabrutinib and found that Btk Y223 phosphorylation was lost at a concentration (3 μ M) that also partially inhibited phosphorylation of Syk (Supplementary Figure 2). This concentration caused a marked reduction on platelet activation by CLEC-2 but no change to platelet aggregation in response to GPVI ligation¹⁶ confirming the selectivity to CLEC-2. The observation, however, of partial phosphorylation of Syk and complete abrogation of phosphorylation of Btk in the presence of acalabrutinib suggests that Btk does not lie upstream of Syk in contrast to the conclusion of Manne *et al*²⁶.

A further prediction in the model of Manne *et al*²⁶ in which Syk lies downstream of Btk is that inhibition of Syk should not block phosphorylation of Btk. To test this, we incubated human platelets with increasing concentrations of the Syk inhibitor PRT 060318 prior to stimulation with rhodocytin. Lysates were then probed using phosphospecific antibodies to Syk pY525/6, LAT pY200, Btk pY551 and PLC γ 2 pY1217. Supplementary Figure 3 shows that phosphorylation of Syk, LAT, Btk and PLC γ 2 were lost in tandem providing further evidence against the model. This result is in keeping with our previous results examining CLEC-2-mediated phosphorylation events in mice with a Syk mutation rendering it unable to undergo tyrosine phosphorylation⁹.

In summary, the above results show that low concentrations of ibrutinib and acalabrutinib selectively block platelet activation by CLEC-2 over GPVI and provide evidence against the model of Manne *et al* in which Btk lies upstream of Syk.

ADP rescues Syk phosphorylation in the presence of Btk inhibition

We have previously shown that CLEC-2 signalling in human platelets is critically dependent on positive feedback signals from thromboxane TP and ADP P2Y₁₂ receptors⁸. Our standard platelet preparation method leads to partial desensitisation of the ADP P2Y₁ receptor²⁷ and loss of aggregation to ADP as a consequence of this (Supplementary Figure 4). This may have accentuated the previously described dependency on P2Y₁₂ receptors. To investigate this, we repeated the studies on aggregation and protein phosphorylation but in the presence of excess ADP (10 μ M). Similar to the results with no added ADP, 70 nM ibrutinib inhibited aggregation (Figure 3Bii) and phosphorylation of Btk Y223 and PLC γ 2 Y1217 (Figure 3Bi-ii). In contrast, however, it did not inhibit phosphorylation of Syk Y525/6, LAT Y200 or Btk on its Src kinase phosphorylation site Y551 (Figure 3Bi and iii). The demonstration of phosphorylation of Syk, LAT and Btk on Y551 but absence of Btk autophosphorylation on Y223 in ibrutinib treated human platelets confirms that Btk lies downstream of Syk in the CLEC-2 signalling cascade in human platelets.

CLEC-2-mediated platelet aggregation and tyrosine phosphorylation is blocked in patients with Btk mutations

Our previous study found off-target effects of ibrutinib even when used at concentrations as low as 70 nM¹⁶. To investigate whether the potent inhibition of CLEC-2-mediated platelet activation by ibrutinib was mediated by its blockade of Btk or an off-target effect, we studied platelet aggregation to rhodocytin in patients with XLA. CLEC-2-mediated aggregation and phosphorylation of PLC γ 2 Y1217 were blocked, whereas phosphorylation of Syk Y525/6 and LAT Y200 was only partially reduced (Figure 4). This demonstrates that the initial phosphorylation of Syk and LAT is independent of Btk and that this is then increased by a Btk-dependent pathway.

The kinase domain of Btk is required for signalling downstream of CLEC-2

We have previously shown that Btk supports platelet activation by GPVI through both

acting as a kinase and as an adapter protein¹⁶. The observation of complete loss of aggregation in the presence of ibrutinib and acalabrutinib however suggests the kinase activity of Btk is critical for activation by CLEC-2. Consistent with this, wild type but not kinase dead (KD) Btk restored NFAT signalling in a CLEC-2 transfected cell line model, which was blocked by ibrutinib and acalabrutinib (Figure 5A-C). CLEC-2 and Btk expression was similar regardless of the Btk construct used (Figure 5D-E). The lack of signalling with KD Btk confirms a fundamental difference between the role of Btk in the CLEC-2 and GPVI signalling pathways.

Btk does not lie upstream of Syk in CLEC-2 stimulated mouse platelets

We extended the studies to investigate the role of Btk in CLEC-2 signalling in mouse platelets. In agreement with the results of Lee *et al*²⁸, we found that only high concentrations of ibrutinib, that abrogated platelet activation by GPVI, blocked CLEC-2-mediated platelet aggregation (Figure 6A, Table 1 and not shown). Phosphorylation of Syk Y519/520 (equivalent to Y525/526 in human platelets), and LAT Y132 and Y200 were preserved in the presence of ibrutinib (Figure 6B). This is consistent with the results in human platelets stimulated by CLEC-2 in the presence of ADP and further confirm that Btk does not lie upstream of Syk and LAT in mouse platelets.

The effect of ibrutinib on deep vein thrombosis

We sought to establish whether ibrutinib would prevent inferior vena cava (IVC) thrombus formation in a mouse model of deep vein thrombosis (DVT) that is known to be dependent on CLEC-2. Mice were dosed with ibrutinib via intraperitoneal injection for up to four days. This dosing strategy blocked CLEC-2-mediated but not PAR4-mediated platelet activation (Figure 7A). Mice dosed with ibrutinib had a reduction in thrombus prevalence relative to controls (Figure 7Bi) but this was not statistically significant. In the small number of ibrutinib treated mice which still formed IVC thrombi, thrombus size was not significantly altered relative to controls (Figure 7Bii).

Discussion

The main findings from the above studies into the role of Btk downstream of CLEC-2 receptor ligation in platelets are (i) Btk lies downstream of Syk in the CLEC-2 signalling cascade in human and mouse platelets in contrast to the conclusion of Manne *et al.*; and (ii) Btk inhibitors selectively block platelet activation by CLEC-2 relatively to GPVI. This suggests that Btk inhibitors can be used to selectively block CLEC-2-mediated platelet activation in thrombo-inflammation without any increase in bleeding or other side effects due to blockade of GPVI and ITAM receptors in other cells.

The results depicted here do not support the conclusions by Manne *et al.* that Btk lies upstream of Syk in CLEC-2 signalling in both human and mouse platelets²⁶. While we were able to replicate the complete loss of whole cell tyrosine, Syk and Btk phosphorylation with ibrutinib in human platelets reported by Manne *et al.*, we show that ibrutinib blocks Btk phosphorylation at its Src phosphorylation site (Y551) which is not in keeping with the known mechanism of action of ibrutinib; Btk is phosphorylated by Src at Y551 but ibrutinib then blocks subsequent autophosphorylation at Y223. We also report of loss of Btk phosphorylation using the Syk inhibitor PRT 060318. Both of these findings are inconsistent with a model in which Btk lies upstream of Syk. This is further supported by the observation that phosphorylation of Syk and Btk Y551 is restored in the presence of the secondary messenger ADP. These results demonstrate that the initial phosphorylation of Syk is independent of Btk and that this is then increased by a pathway that involves Btk and ADP.

Our results show that human CLEC-2-mediated platelet activation is critically dependent on the kinase function of Btk. Low concentrations of ibrutinib and the more Btk-selective acalabrutinib, as well as patients treated with these inhibitors and patients with genetic loss-of-function mutations of Btk, have no demonstrable CLEC-2-mediated platelet activation, even when stimulated with very high levels of agonist. We have previously shown that genetic or pharmacological Btk inhibition of platelets does not result in loss of activation to GPVI in human platelets because; (i) Btk was able to function as an adapter downstream of GPVI to preserve platelet activation and (ii) Tec may be able to compensate for the lack of Btk kinase or adapter activity¹⁶. Here we show that Tec is not able to compensate for a lack of Btk in the CLEC-2 signalling cascade through studies on patients with XLA and that the kinase domain of Btk is critical for CLEC-2's signalling in a transfected cell line model.

The present results suggest that Btk inhibitors have the potential to be used at very low concentrations as selective inhibitors of CLEC-2 in thrombo-inflammatory disorders with minimal off-target effects and no increased bleeding. Not only does Btk inhibition prevent platelet activation to CLEC-2 but we have shown that it also results in abrogation of platelet adhesion to podoplanin at venous rates of shear and a reduction in DVT formation in the ibrutinib treated mice. The *in vivo* DVT study was powered based on the rates of thrombosis seen in CLEC-2 deficient and WT mice in the studies of Payne *et al.*⁸. The lack of statistical significance in the trend towards inhibition of DVT formation may reflect the fact that pharmacological blockade of Btk in mice did not result in full inhibition of CLEC-2 signalling throughout the 48 hours required for venous thrombosis in this model and the fact that, unlike for human CLEC-2 signalling, mouse CLEC-2 is not critically dependent on Btk. Interestingly the thrombi that did form in the ibrutinib-treated mice were the same size as in the control mice. This is consistent with a model where CLEC-2 activation is required to initiate thrombus formation, but not to propagate it.

Conclusion

In conclusion, the present study shows that Btk lies downstream of Syk in human and mouse platelets and shows that Btk inhibitors block human CLEC-2-mediated platelet function at >20-fold lower concentrations than they block GPVI signalling¹⁶ and mouse CLEC-2. The mechanism underlying this selectivity is because Btk kinase activity is critical for human platelet CLEC-2 function, but not for GPVI. This means that low dose Btk inhibitors could be used therapeutically to inhibit CLEC-2 in platelets without any off-target effects on GPVI and ITAM receptors in other haematopoietic cells. This provides a mechanism for selective targeting of CLEC-2 in thrombo-inflammatory disorders, such as DVT or infection-driven thrombosis, whilst preserving haemostasis^{3,4}.

References

1. Lowe K, Watson SP, Lax S, Frampton J. CLEC-2 is not required to maintain separation of intact blood and lymphatic vasculature. *Blood*. 2015;123(20):3200-3207.
2. Astarita JL, Acton SE, Turley SJ. Podoplanin: emerging functions in development, the immune system, and cancer. *Front Immunol*. 2012;3(283):1-11.
3. Payne H, Ponomaryov T, Watson SP, Brill A. Mice with a deficiency in CLEC-2 are protected against deep vein thrombosis. *Blood*. 2017;129(14):2013-2020.
4. Hitchcock JR, Cook CN, Bobat S, et al. Inflammation drives thrombosis after Salmonella infection via CLEC-2 on platelets. *J Clin Invest*. 2015;125(12):4429-4446.
5. Rayes J, Watson SP, Nieswandt B. Functional significance of the platelet immune receptors GPVI and CLEC-2. *J Clin Invest*. 2019;129(1):12-23.
6. Severin S, Pollitt AY, Navarro-Núñez L, et al. Syk-dependent Phosphorylation of CLEC-2: A novel mechanism of hem-immunoreceptor tyrosine-based activation motif signaling. *J Biol Chem*. 201;286(6):4107-4116.
7. Spalton JC, Mori J, Pollitt AY, Hughes CE, Eble JA, Watson SP. The novel Syk inhibitor R406 reveals mechanistic differences in the initiation of GPVI and CLEC-2 signaling in platelets. *J Thromb Haemost*. 2009;7(7):1192-1199.
8. Pollitt AY, Grygielska B, Leblond B, Desire L, Eble JA, Watson SP. Phosphorylation of CLEC-2 is dependent on lipid rafts, actin polymerization, secondary mediators, and Rac. *Blood*. 2010;115(14):2938-2946.
9. Hughes CE, Finney BA, Koentgen F, Lowe KL, Watson SP. The N-terminal SH2 domain of Syk is required for (hem)ITAM, but not integrin, signaling in mouse platelets. *Blood*. 2015;125(1):144-154.
10. Fuller G, Williams J, Tomlinson MG, et al. The C-type Lectin Receptors CLEC-2 and Dectin-1, but Not DC-SIGN, Signal via a Novel YXXL-dependent Signaling Cascade. *J Biol Chem*. 2007;282(17):12397-12409.
11. Hughes CE, Pollitt AY, Mori J, et al. CLEC-2 activates Syk through dimerization. *Blood*. 2010;115(14):2947-2955.
12. Borgognone A, Navarro-Núñez L, Correia JN, et al. CLEC-2-dependent activation of mouse platelets is weakly inhibited by cAMP but not by cGMP. *J Thromb Haemost*. 2014;12(4):550-559.

13. Byrd JC, Furman RR, Coutre SE, et al. Targeting BTK with Ibrutinib in Relapsed Chronic Lymphocytic Leukemia. *N Engl J Med*. 2013;369(1):32-42.
14. Byrd JC, Harrington B, O'Brien S, et al. Acalabrutinib (ACP-196) in Relapsed Chronic Lymphocytic Leukemia. *N Engl J Med*. 2016;374(4):323-332.
15. Wang M, Rule S, Zinzani PL, et al. Acalabrutinib in relapsed or refractory mantle cell lymphoma (ACE-LY-004): a single-arm, multicentre, phase 2 trial. *Lancet*. 2018;391(10121):659-667.
16. Nicolson PLR, Hughes CE, Watson S, et al. Inhibition of Btk by Btk-specific concentrations of ibrutinib and acalabrutinib delays but does not block platelet aggregation to GPVI. *Haematologica*. 2018;103(12):2097-2108.
17. Burkhardt JM, Vaudel M, Gambaryan S, et al. The first comprehensive and quantitative analysis of human platelet protein composition allows the comparative analysis of structural and functional pathways. *Blood*. 2012;120(15):e73-82.
18. Zeiler M, Moser M, Mann M. Copy Number Analysis of the Murine Platelet Proteome Spanning the Complete Abundance Range. *Mol Cell Proteomics*. 2014;13(12):3435-3445.
19. Quek LS, Bolen J, Watson SP. A role for Bruton's tyrosine kinase (Btk) in platelet activation by collagen. *Curr Biol*. 1998;8(20):1137-1140.
20. Atkinson BT, Ellmeier W, Watson SP. Tec regulates platelet activation by GPVI in the absence of Btk. *Blood*. 2003;102(10):3592-3599.
21. Busygina K, Denzinger V, Bernlochner I, Weber C, Lorenz R, Siess W. Btk Inhibitors as First Oral Atherothrombosis-Selective Antiplatelet Drugs? *Thromb Haemost*. 2019;119(08):1212-1221.
22. Levade M, David E, Garcia C, et al. Ibrutinib treatment affects collagen and von Willebrand factor-dependent platelet functions. *Blood*. 2014;124(26):3991-3995.
23. Kamel S, Horton L, Ysebaert L, et al. Ibrutinib inhibits collagen-mediated but not ADP-mediated platelet aggregation. *Leukemia*. 2015;29(4):783-787.
24. Bye AP, Unsworth AJ, Desborough MJ, et al. Severe platelet dysfunction in NHL patients receiving ibrutinib is absent in patients receiving acalabrutinib. *Blood Adv*. 2017;1(26):2610-2623.
25. Busygina K, Jamasbi J, Seiler T, et al. Oral Bruton tyrosine kinase inhibitors selectively block atherosclerotic plaque-triggered thrombus formation in humans. *Blood*. 2018;131(24):2605-2616.
26. Manne BK, Badolia R, Dangelmaier C, et al. Distinct Pathways Regulate Syk Protein Activation Downstream of Immune Tyrosine Activation Motif (ITAM) and hemITAM Receptors in Platelets. *J Biol Chem*. 2015;290(18):11557-11568.
27. Koessler J, Hermann S, Wener K, et al. Role of Purinergic Receptor Expression and Function for Reduced Responsiveness to Adenosine Diphosphate in Washed Human Platelets. *PLoS One*. 2016; 11(1):e0147370.
28. Lee RH, Piatt R, Conley PB, Bergmeier W. Effects of ibrutinib treatment on murine platelet function during inflammation and in primary hemostasis. *Haematologica*. 2017;102(3):e89-e92.

29. Gitz E, Pollitt AY, Gitz-Francois JJ, et al. CLEC-2 expression is maintained on activated platelets and on platelet microparticles. *Blood*. 2014;124(14):2262-2270.
30. Suzuki-Inoue K, Fuller G, Garcia A, et al. A novel Syk-dependent mechanism of platelet activation by the C-type lectin receptor CLEC-2. *Blood*. 2006;107(2):542-549.
31. Navarro-Núñez L, Pollitt AY, Lowe K, Latif A, Nash GB, Watson SP. Platelet adhesion to podoplanin under flow is mediated by the receptor CLEC-2 and stabilised by Src/Syk-dependent platelet signalling. *Thromb Haemost*. 2015;113(5):1109-1120.
32. Fillbrunn A, Dietz C, Pfeuffer J, Rahn R, Landrum GA, Berthold MR. KNIME for reproducible cross-domain analysis of life science data. *J Biotechnol*. 2017;261:149-156.
33. Sommer C, Straehle C, Kothe U, Hamprecht FA. Ilastik: Interactive learning and segmentation toolkit. 2011 IEEE International Symposium on Biomedical Imaging: From Nano to Macro. IEEE. 2011:230-233.

Table and Figure Legends

Figure	Dose Response Curve	IC ₅₀ (μM)	95% C.I.
1B	HD Aggregation	0.023	0.009 — 0.053
3Aii	HD Btk pY223	0.024	0.002 — 0.133
3Aii	HD PLCγ2 pY1217	0.034	0.010 — 0.119
3Aiii	HD Syk pY525/6	0.052	0.020 — 0.150
3Aiii	HD LAT pY200	0.036	0.028 — 0.189
3Aiii	HD SLP76 pY145	0.032	0.015 — 0.066
3Aiii	HD Btk pY551	0.059	0.023 — 0.179
3Aiv	HD Src pY418	-	-
3Bii	HD Aggregation (added 10 μM ADP)	0.034	0.017 — 0.07
3Biii	HD Btk pY223 (added 10 μM ADP)	0.006	0.003 — 0.009
3Biii	HD PLCγ2 pY1217 (added 10 μM ADP)	0.023	0.014 — 0.037
6B	WT Mouse WP Aggregation	13.28	4.650 — 129.2
6Bii	WT Mouse Btk pY223	0.076	0.011 — 0.559
6Bii	WT Mouse PLCγ2 Y753	0.074	0.026 — 0.200
6Bii	WT Mouse PLCγ2 Y759	0.065	0.017 — 0.232
6Bii	WT Mouse PLCγ2 Y1217	0.122	0.044 — 0.363
6Biii	WT Mouse Syk pY525/6	-	-
6Biii	WT Mouse LAT pY132	-	-
6Biii	WT Mouse LAT pY200	-	-
6Biii	WT Mouse Btk pY551	-	-
6Biv	WT Mouse Src pY418	0.35	0.126 — 1.036

Table 1: IC₅₀ values for all dose response curves shown in figures in this study. Where no value is shown this indicates that the IC₅₀ could not be calculated.

Figure 1: Btk inhibitors completely block CLEC-2 mediated platelet aggregation *in vitro* and *ex vivo*. Washed platelets at 4×10^8 /ml isolated from healthy donors (HD) were stimulated with 300 nM rhodocytin after incubation with ibrutinib or vehicle at the stated doses for 5 minutes. LTA measurements were then undertaken for 5 minutes. (A) Representative traces of three identical aggregation experiments. (B) Dose response curves (n=3). (C) PRP was isolated from the blood of patients with CLL following treatment with FCR, ibrutinib or acalabrutinib based chemotherapy regimens. (i) Representative trace and (ii) mean \pm SEM (post-FCR n=5, post-ibrutinib n=12, post-acalabrutinib n=3) of optical density 5 minutes after stimulation with rhodocytin 10 – 300 nM. All results are shown as mean \pm SEM. Statistical analysis was performed with a 2-way ANOVA with Tukey's correction for multiple comparisons. *P<0.05, ns = non-significant.

Figure 2: Btk inhibition blocks platelet adhesion to podoplanin under venous flow

conditions. Whole blood from healthy donors, patients treated with ibrutinib or acalabrutinib or those with XLA was incubated with DiOC₆ dye for 5 minutes before being flowed across a capillary coated with podoplanin-Fc (100 µg/ml) at 125 s⁻¹ for 5 minutes. Images were taken every second using fluorescent channels on a Zeiss Axio inverted microscope at 20X magnification. (A) Representative images from (i) healthy donors, patients treated with (ii) ibrutinib 420 mg once daily, (iii) acalabrutinib 100 mg twice daily or (iv) patients with XLA. Ilastik 1.1.2 machine learning software was used to automatically and reproducibly identify platelets. Data on platelet surface area coverage and cluster size was measured using the KNIME 3.4 analytics platform. Mean data ± SEM showing increase in total platelet aggregate area over time of (C) healthy donors (n=4) and ibrutinib treated patients (n=5) and (D) acalabrutinib treated patients (n=2) and those with XLA (n=2). Mean data ± SEM showing increase in mean aggregate size over time of (E) healthy donors and ibrutinib treated patients and (F) acalabrutinib treated patients and those with XLA, the curve from healthy donor platelets is included for comparison. Statistical analysis was performed with two-way ANOVA. *P<0.05, ns=non significant.

Figure 3: Low concentrations of ibrutinib block all phosphorylation events downstream of platelet CLEC-2 ligation, blockade upstream of Btk pY223 is rescued by addition of excess ADP. Healthy donor washed human platelets at 4x10⁸/ml in the presence of eptifibatide 9 µM were incubated with ibrutinib or vehicle for 5 minutes without (A) or with (B) ADP at 10µM prior to stimulation with 300 nM rhodocytin. Platelets were then lysed with 5X reducing sample buffer 5 minutes after addition of agonist. Whole cell lysates were then separated by SDS-PAGE and western blots were probed for whole cell phosphorylation or kinase phosphorylation with the stated antibodies downstream of the platelet CLEC-2 receptor. Representative blot from 4 identical experiments (i). Mean tyrosine levels phosphorylation level ± SEM of 4 identical experiments for phosphorylation events downstream (ii) and upstream (iii) of Btk pY223 as well as Src pY418 (iv). Mean aggregation trace from Figure 1B is included as a dotted line to aid comparison. Mean ± SEM of 3 identical experiments for LTA measurements in the presence of ADP 5 minutes after stimulation with 300 nM rhodocytin are shown as a dotted line in (ii) and (iii).

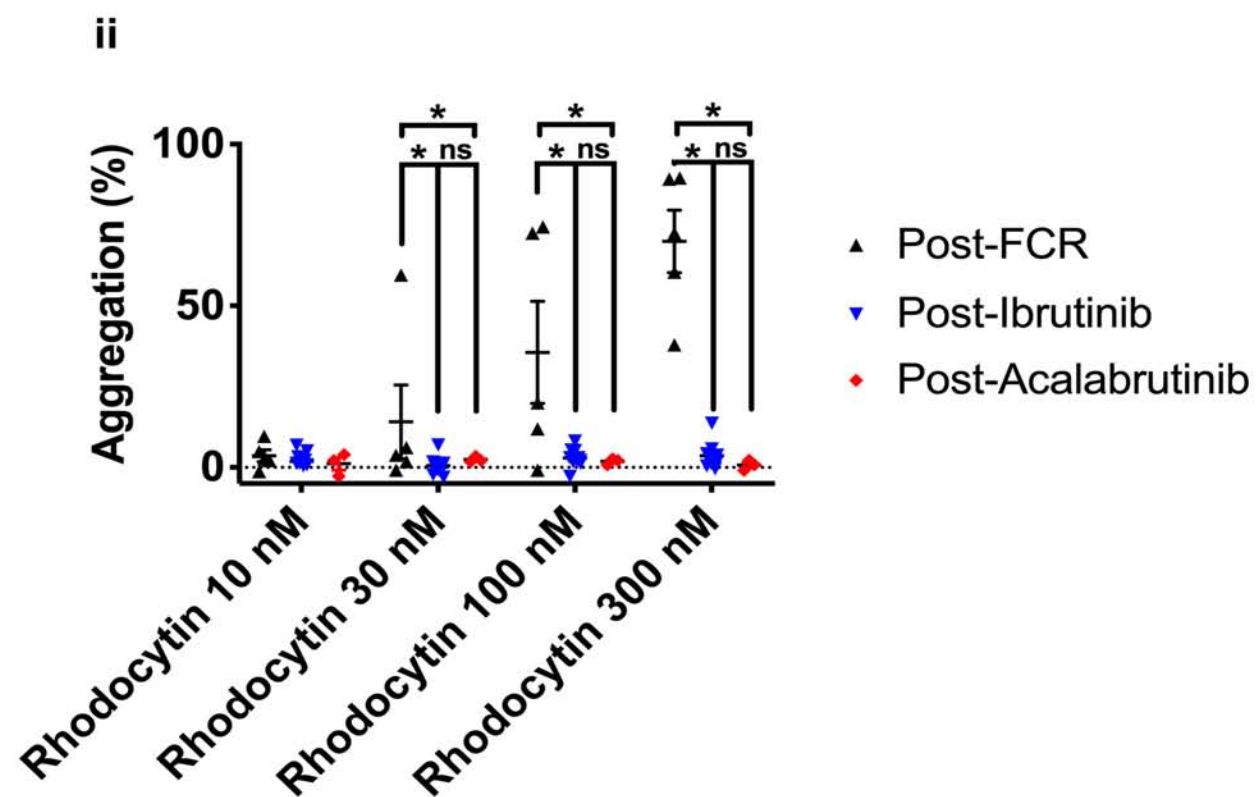
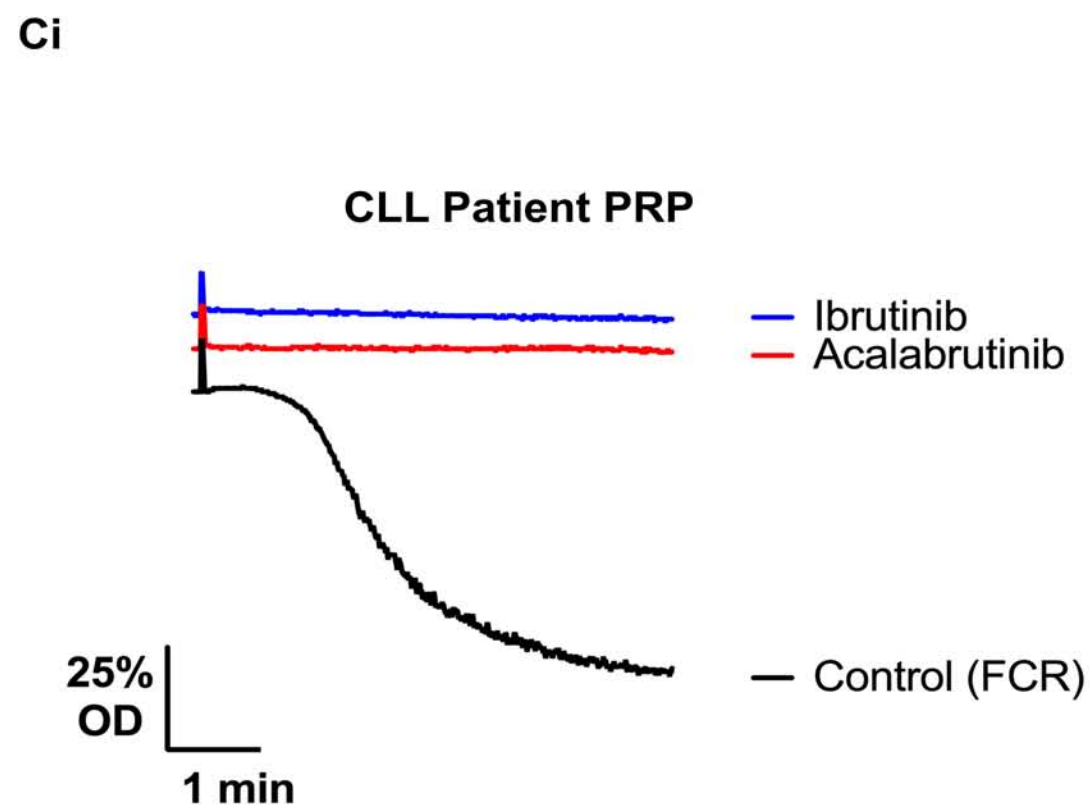
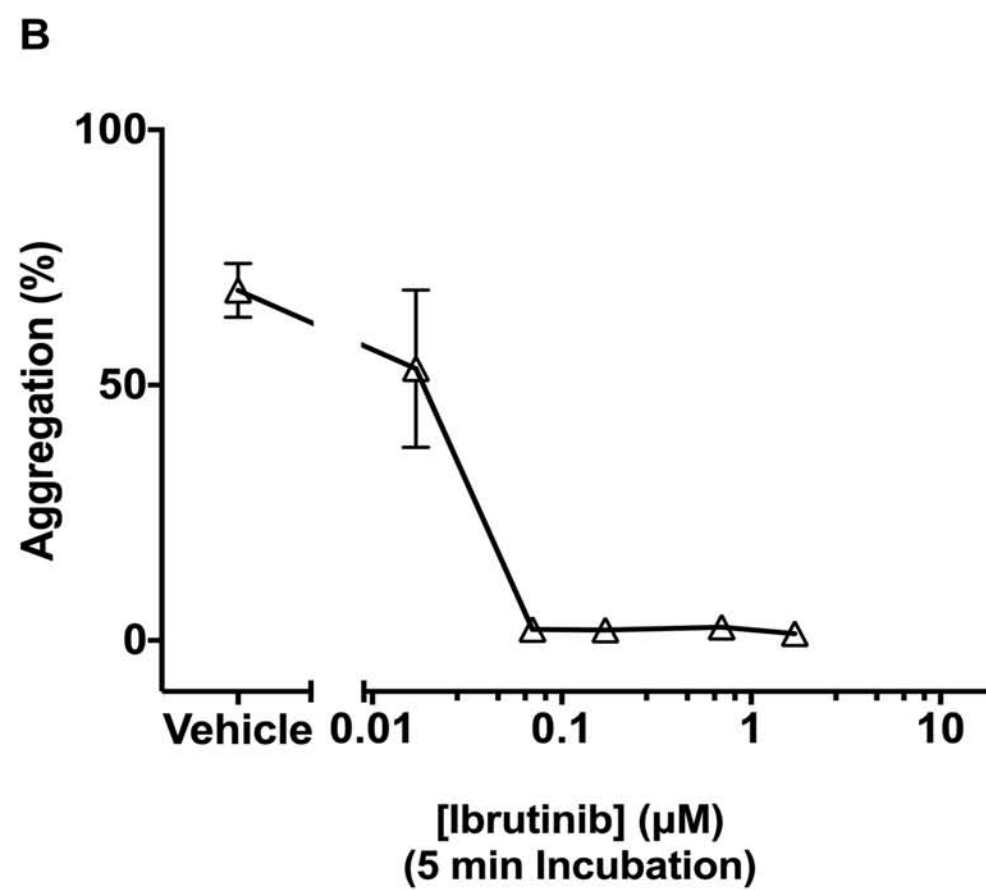
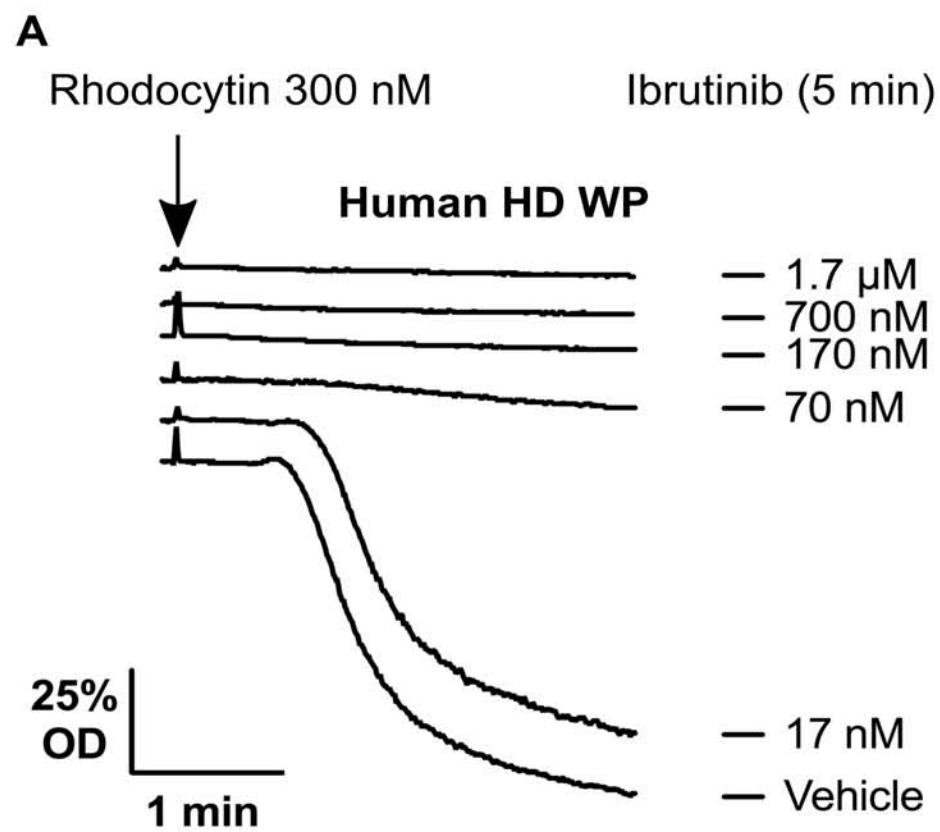
Figure 4: Platelets from patients with XLA do not aggregate in response to ligation of CLEC-2, but signalling events upstream of Btk are partially preserved. (A) PRP was isolated from the blood of patients with XLA and stimulated with rhodocytin. (i) Representative trace and (ii) mean ± SEM (healthy donor n=6, XLA n=4) of optical density 5 minutes after stimulation with rhodocytin 300 nM. Statistical analysis was performed with a two-tailed t-test. (B) Eptifibatide (9 µM) treated washed platelets at 4x10⁸/ml from patients with XLA were lysed with 5X reducing sample buffer 5 minutes after addition of rhodocytin 300 nM or PBS as shown. Whole cell lysates were then separated by SDS-PAGE and western blots were probed for whole cell or tyrosine phosphorylation with the stated antibodies. (i) Blot and (ii) mean ± SEM (n=3) for phosphorylation events downstream of the CLEC-2 receptor. Results were analysed statistically using a one-way ANOVA with Sidak's correction for multiple comparisons.

Figure 5: NFAT luciferase activity in Btk deficient DT40 cells is restored with transfection of WT but not KD Btk. Btk deficient DT40 cells were transfected with either wild type (WT) or kinase dead (KD) Btk with or without CLEC-2. All cells were transfected with a NFAT-luciferase reporter plasmid. Cells were stimulated with rhodocytin 300 nM in the presence of serum. (A) Luciferase activity was measured and is shown as mean ± SEM of five identical experiments. Cells were stimulated with rhodocytin 50 nM in the presence or absence of (B) ibrutinib (0.5 – 10 µM) and (C) acalabrutinib (0.5 – 10 µM). Serum was excluded during stimulation to avoid plasma binding of the drugs. Luciferase activity between vehicle and drug treated samples was measured and is shown as the mean ± SEM

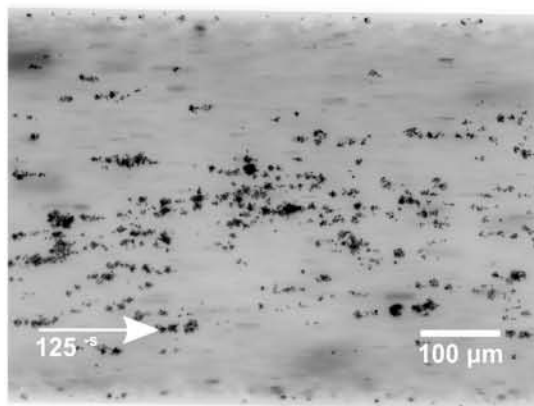
of three independent experiments. (D) CLEC-2 expression in the different transfection conditions. (E) Representative western blot showing Btk expression levels in cells transfected with different Btk constructs (n=5). *P<0.05, ns = non-significant.

Figure 6: Ibrutinib blocks CLEC-2 mediated tyrosine phosphorylation of Btk pY223 at low concentrations in mouse platelets. Aggregation is only blocked at ~250-fold higher concentrations. (A) WT mouse washed platelets at $4 \times 10^8/\text{ml}$ were incubated with vehicle or ibrutinib for 5 minutes prior to stimulation with rhodocytin 300 nM for 5 minutes. Representative trace of LTA is shown from 3 identical experiments. (B) Eptifibatide (9 μM) treated WT mouse washed platelets at $4 \times 10^8/\text{ml}$ were incubated with ibrutinib or vehicle for 5 minutes before being stimulated with rhodocytin 300 nM. Platelets were then lysed with 5X reducing sample buffer 5 minutes after addition of agonist. Whole cell lysates were then separated by SDS-PAGE and western blots were probed for whole cell phosphorylation or kinase phosphorylation with the stated antibodies downstream of the platelet CLEC-2 receptor. (i) Representative blots and (ii-iv) mean results of three identical experiments examining degree of aggregation and tyrosine phosphorylation levels of the proteins shown. Mean aggregation (n=3) results are shown in (ii) and are included as dotted line in (iii-iv) to aid comparison. All results are shown as mean \pm SEM.

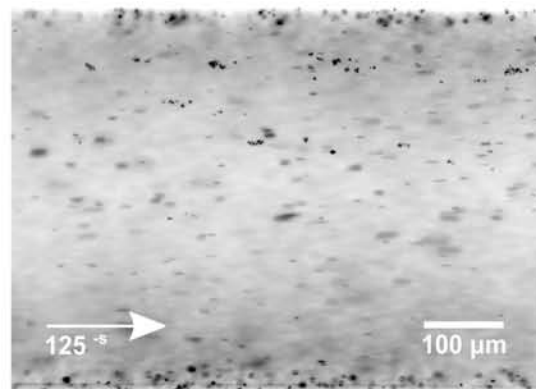
Figure 7: Mice dosed with ibrutinib have a trend towards reduction of thrombus formation in an *in vivo* venous thrombosis model. WT mice were dosed with ibrutinib (35 – 70 mg/kg) or vehicle for 1 – 3 days before and 2 days following IVC stenosis surgery to achieve consistent CLEC-2 inhibition throughout the post-surgical period. (A) Heparinised whole blood was taken via tail bleeding from mice undergoing the same dosing schedule but not undergoing surgery at the stated time points. It was incubated with FITC-conjugated anti-P-selectin and PE-conjugated anti-activated integrin $\alpha\text{IIb}\beta 3$ antibodies for 30 minutes before undergoing red cell lysis and fixation and analysis using flow cytometry. Effect on platelet activation after stimulation with PAR4 peptide (500 nM) and rhodocytin (300 nM) is shown (i) representative plots, (ii) mean data \pm SEM (ibrutinib n=6, vehicle n=3). (B) Two hours following the pre-surgical dose of ibrutinib or vehicle IVC stenosis was induced under general anaesthesia with a ligature. Mice were allowed to recover and were then culled 48 hours later and examined for the size of any IVC thrombus. (i) Thrombus prevalence and (ii) Thrombus length are shown (ibrutinib n=13, vehicle n=12). Horizontal line represents median thrombus length. Statistical analysis on thrombus prevalence was done with Fisher's exact test. Statistical analysis for thrombus length was performed with Mann-Whitney test. ns=non-significant.



Ai

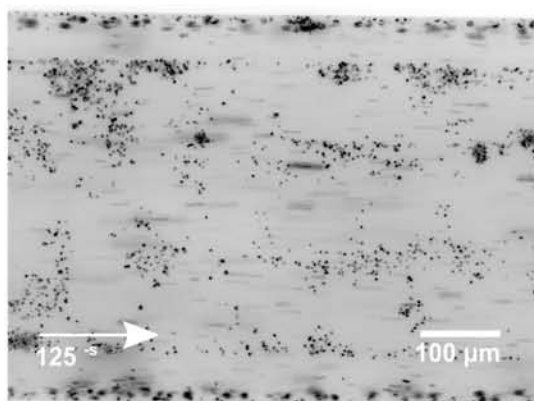


ii



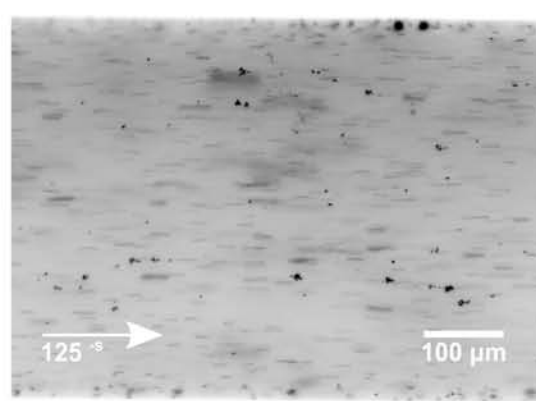
Bi

Healthy Donor



ii

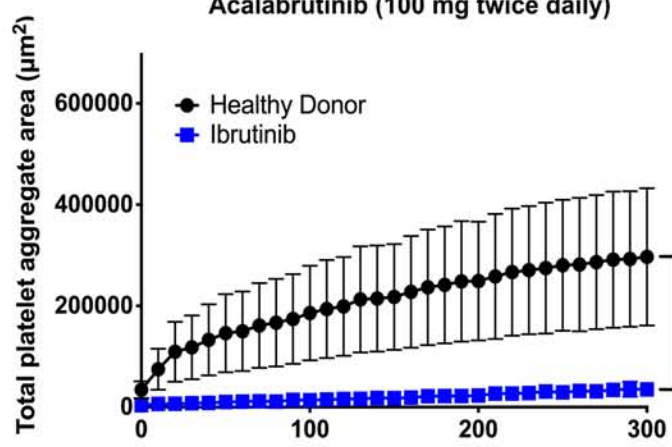
Ibrutinib (420 mg once daily)



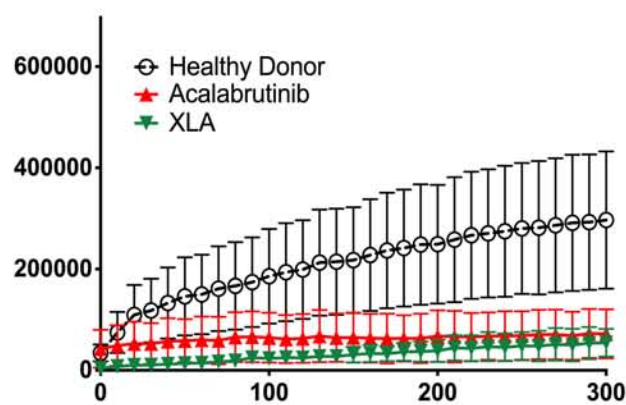
Acalabrutinib (100 mg twice daily)

XLA

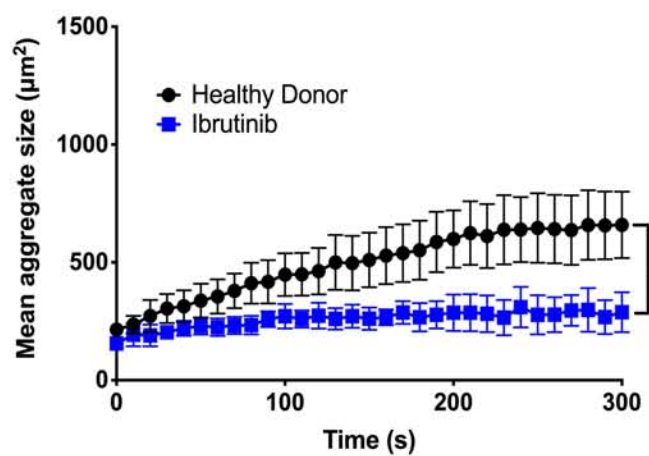
C



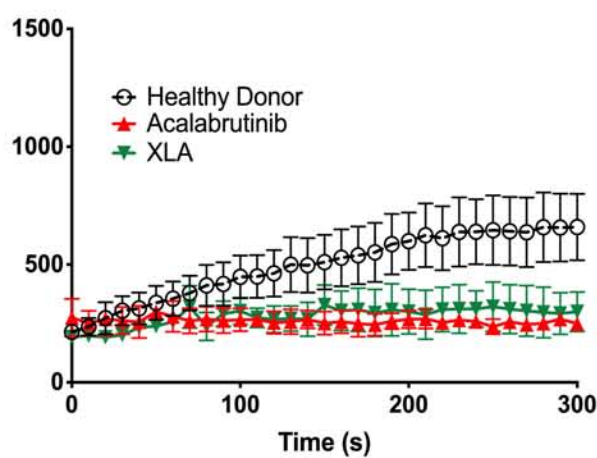
D



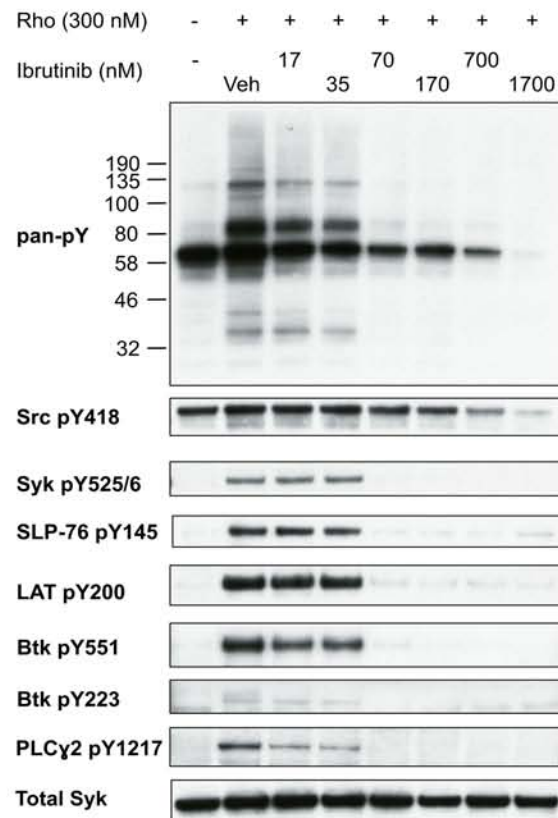
E



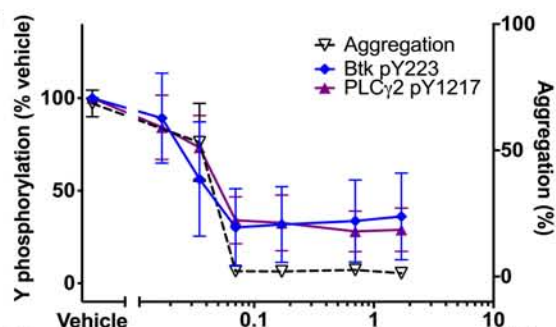
F



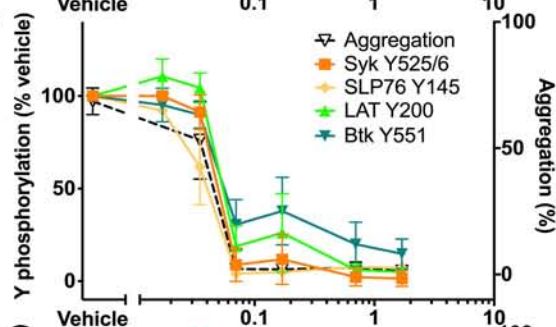
Ai



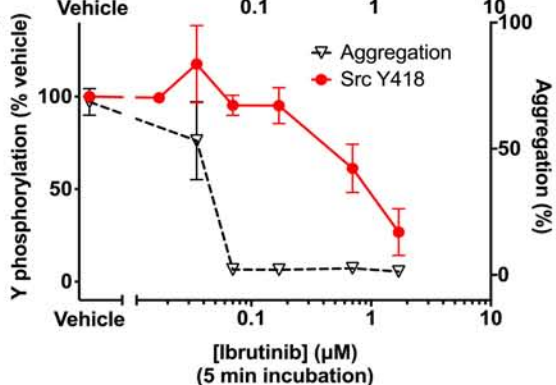
ii



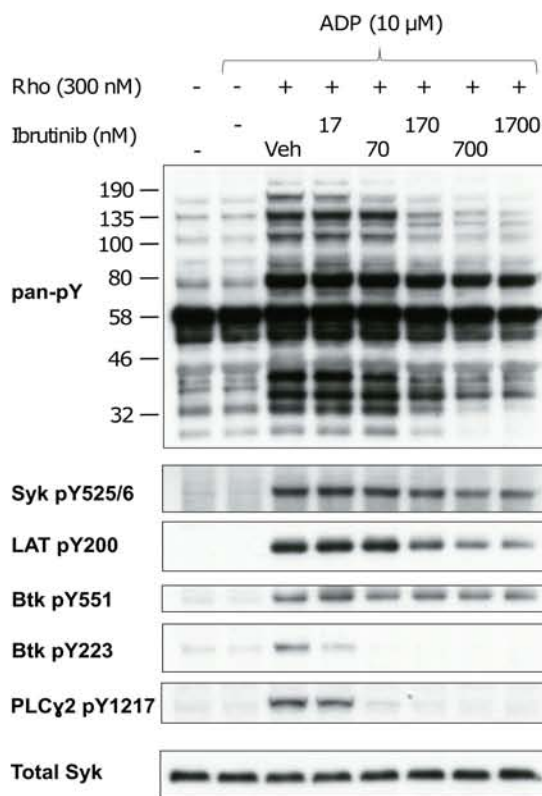
iii



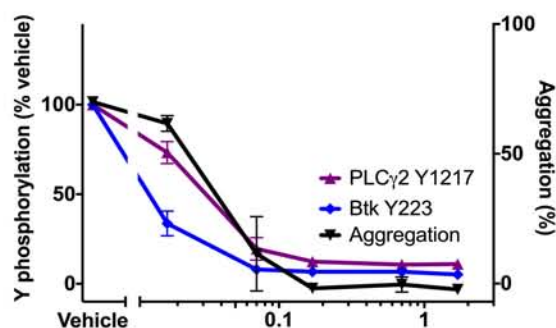
iv



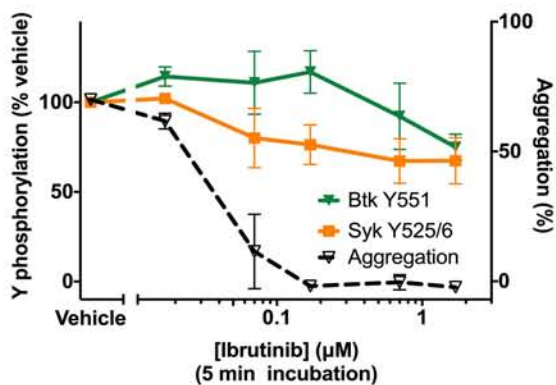
Bi

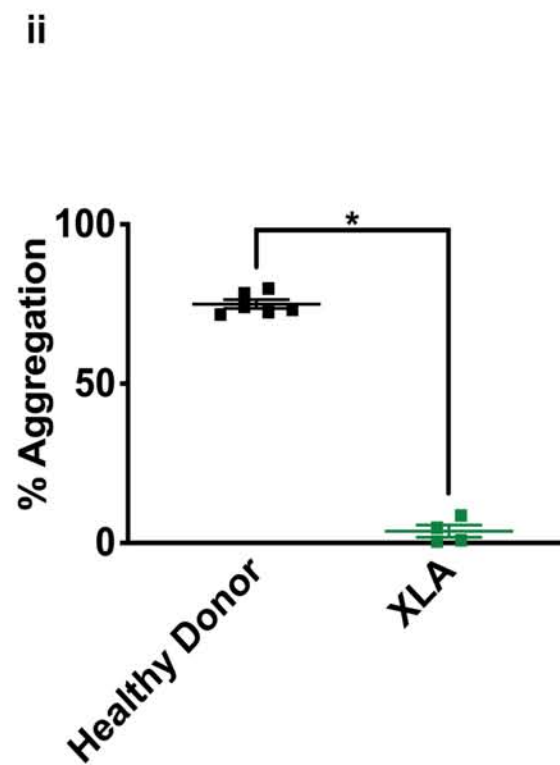
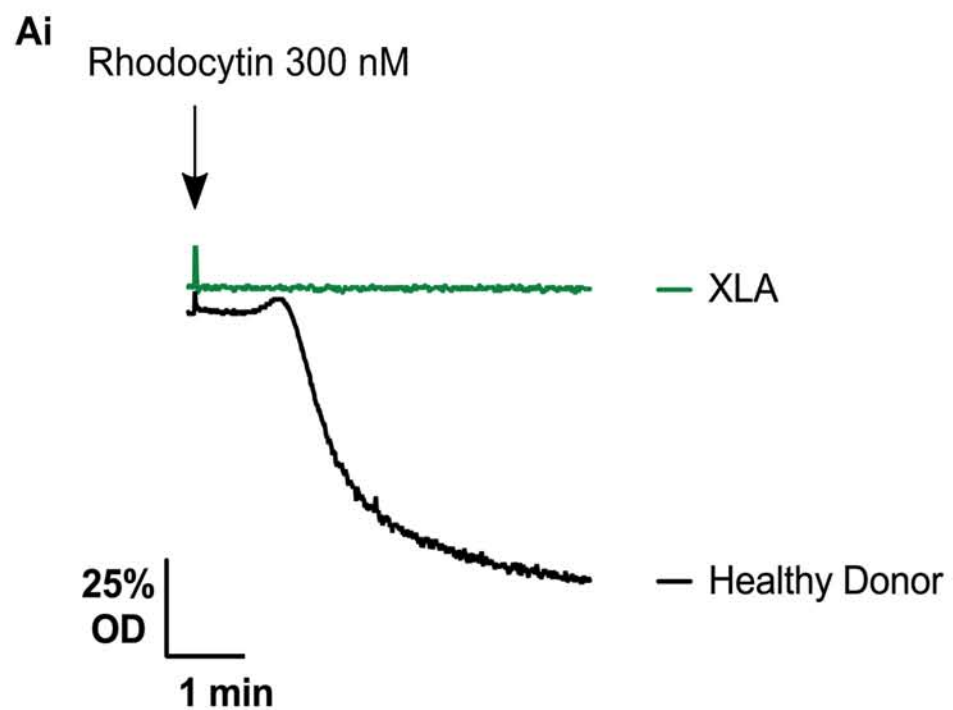


ii



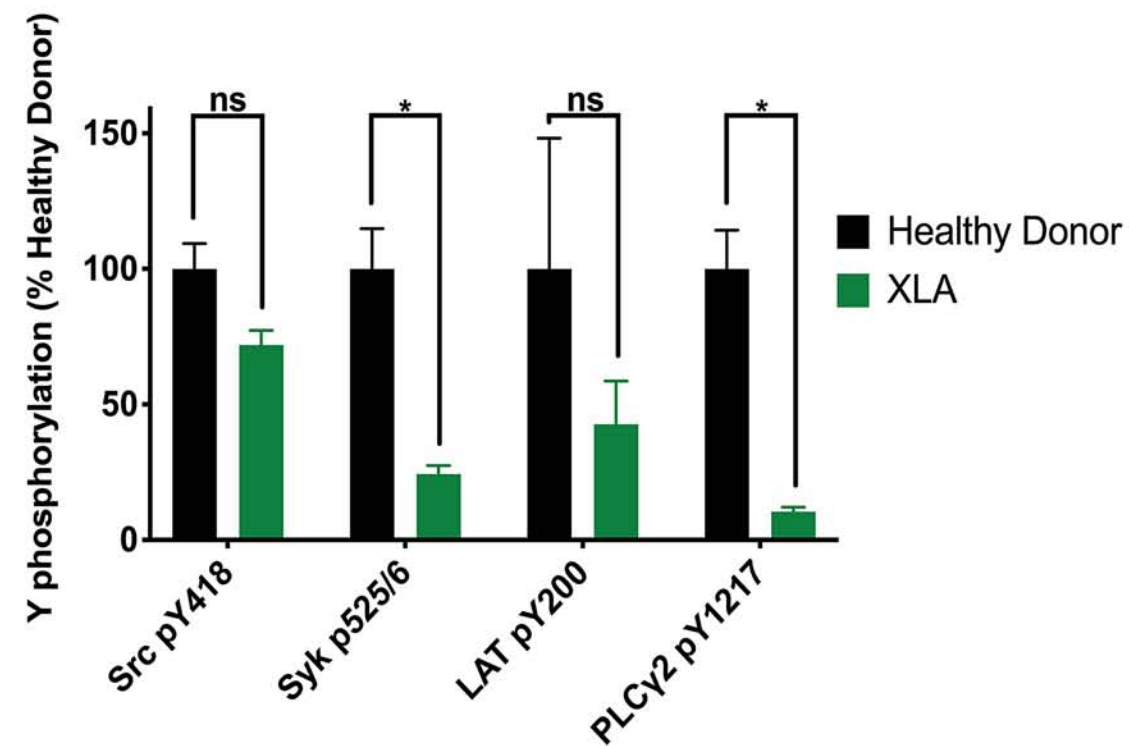
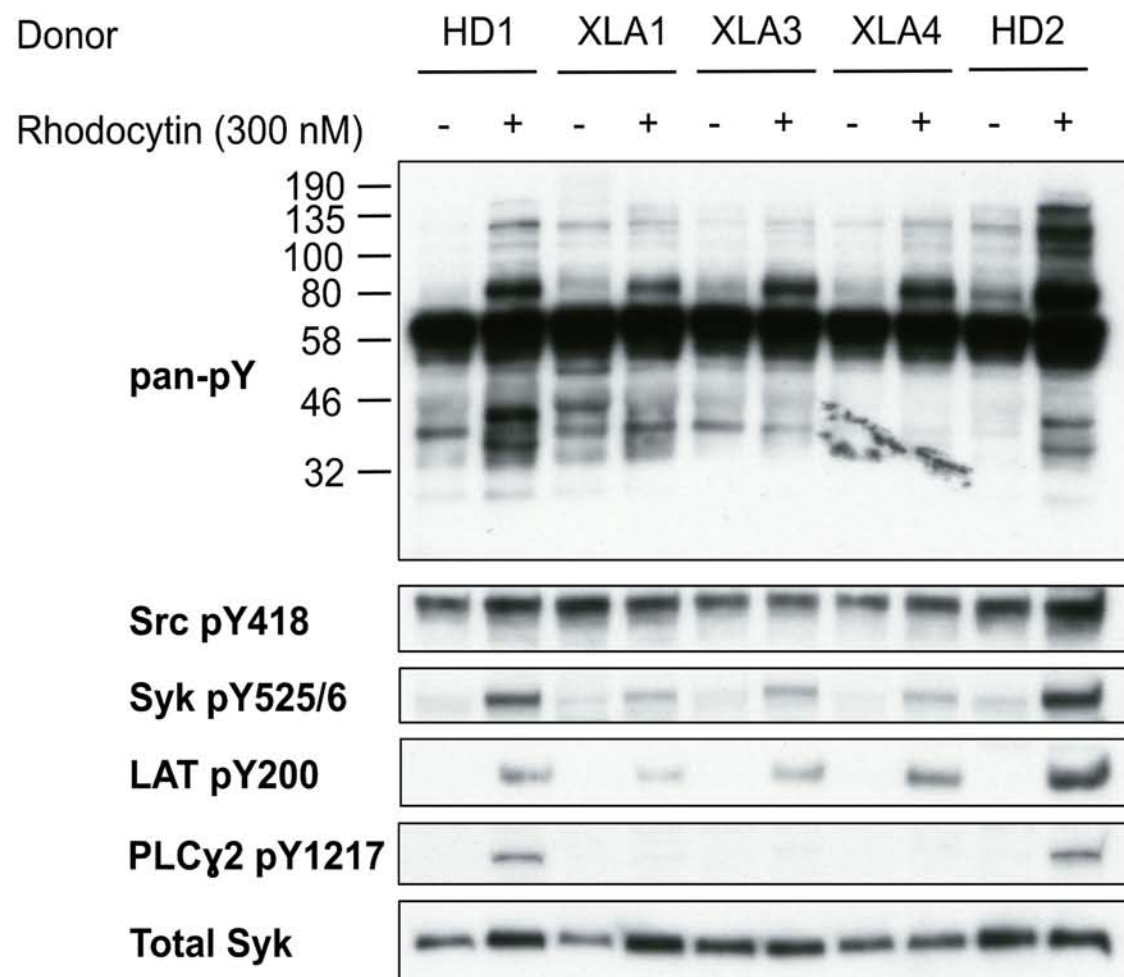
iii

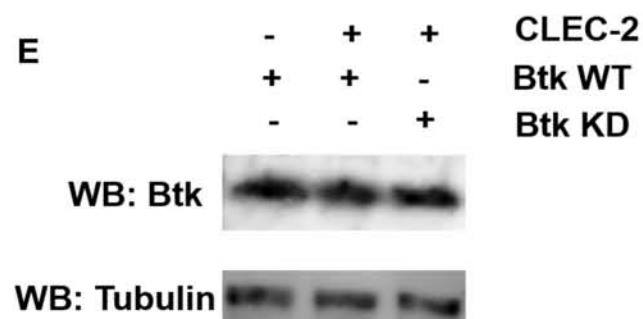
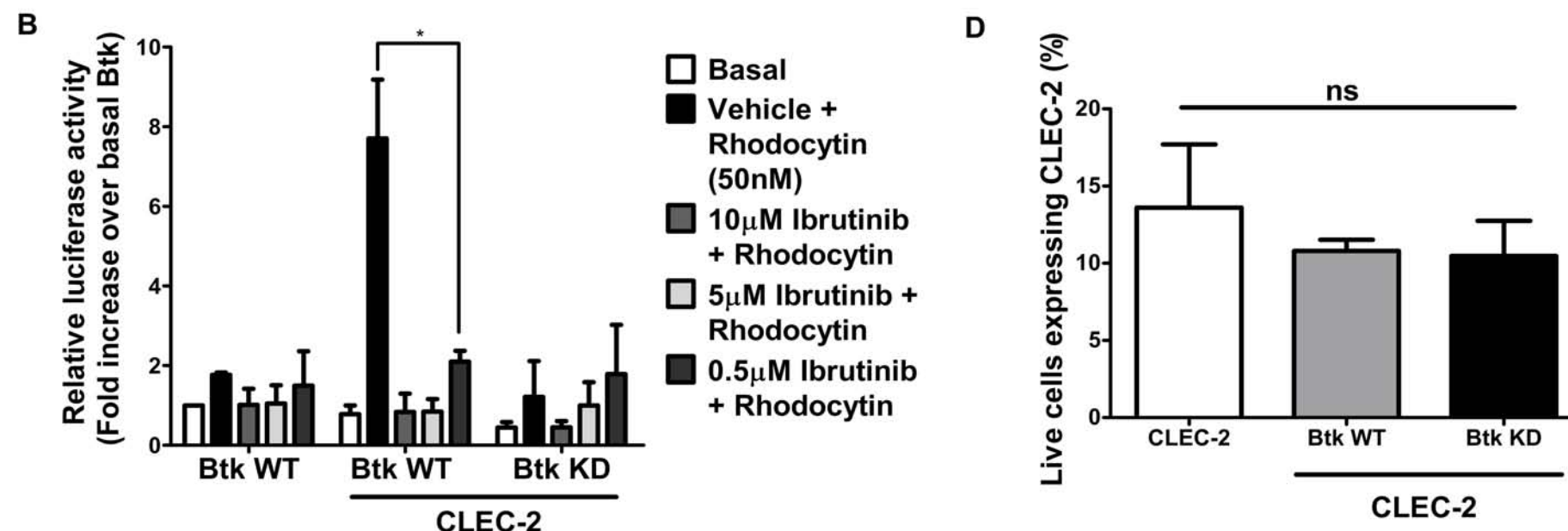
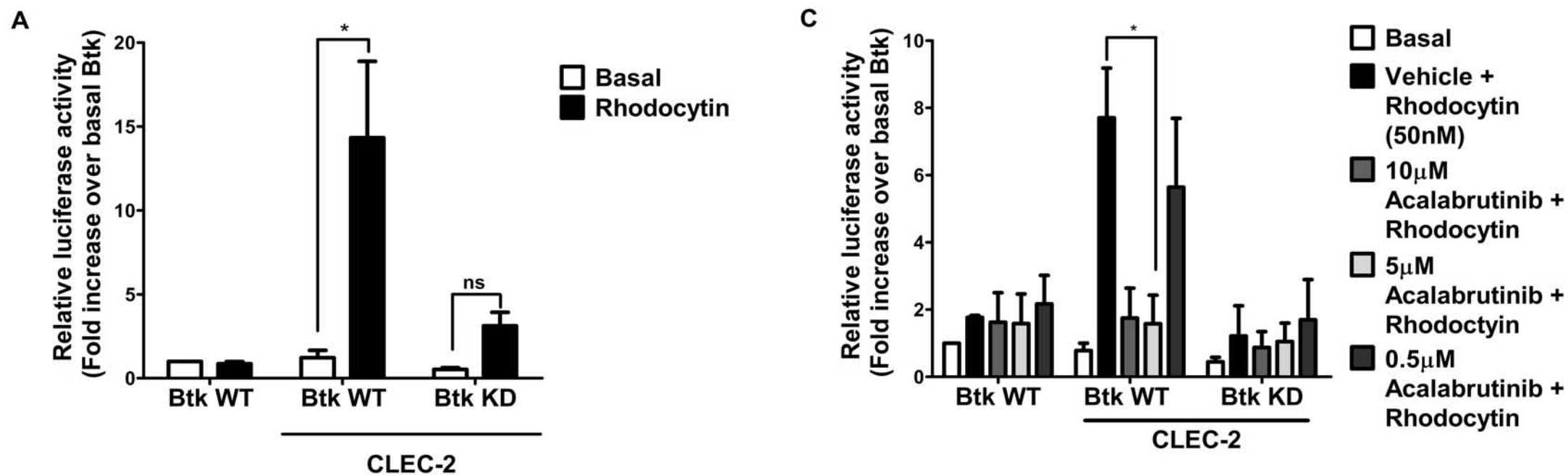




ii

Bi

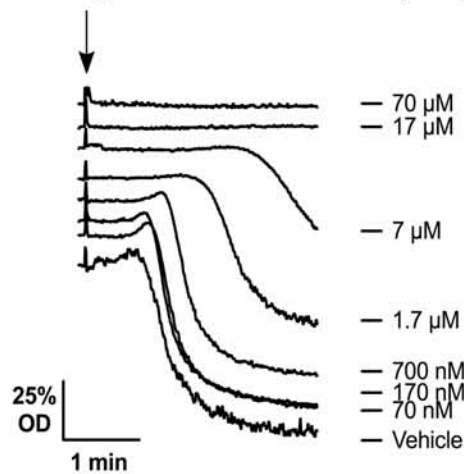




A

Rhodocytin 300 nM

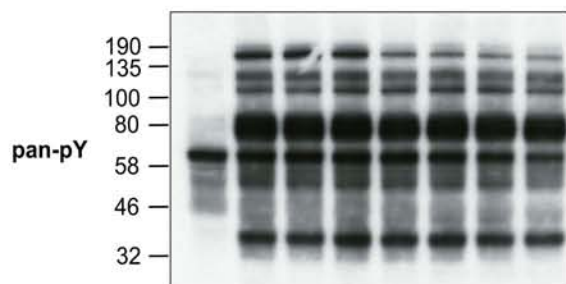
Ibrutinib (5 min)



Mouse platelets

Bi

Rhodocytin (300 nM) - + + + + + + +
 Ibrutinib (nM) - - 17 70 170 700 1700 7000
 Veh



Src pY418



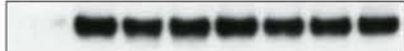
Syk pY519/520



LAT pY132



LAT pY200



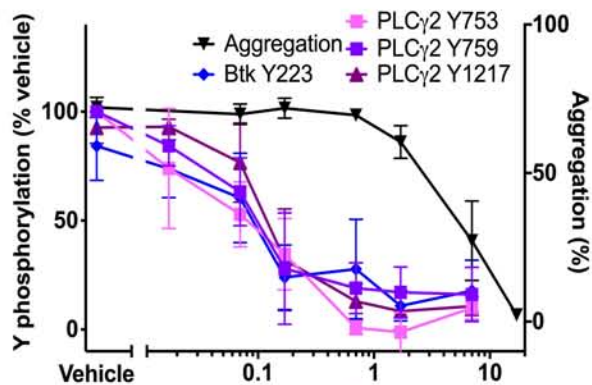
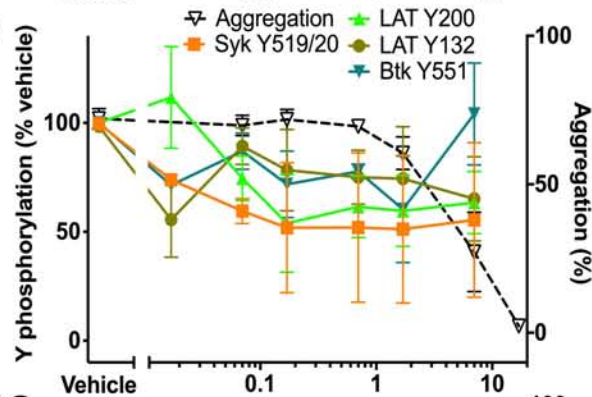
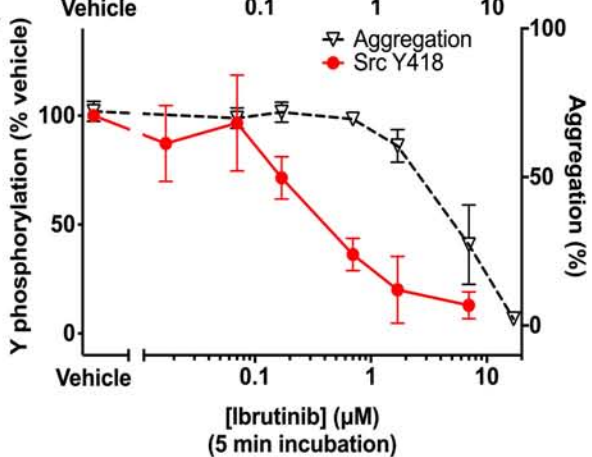
Btk pY551



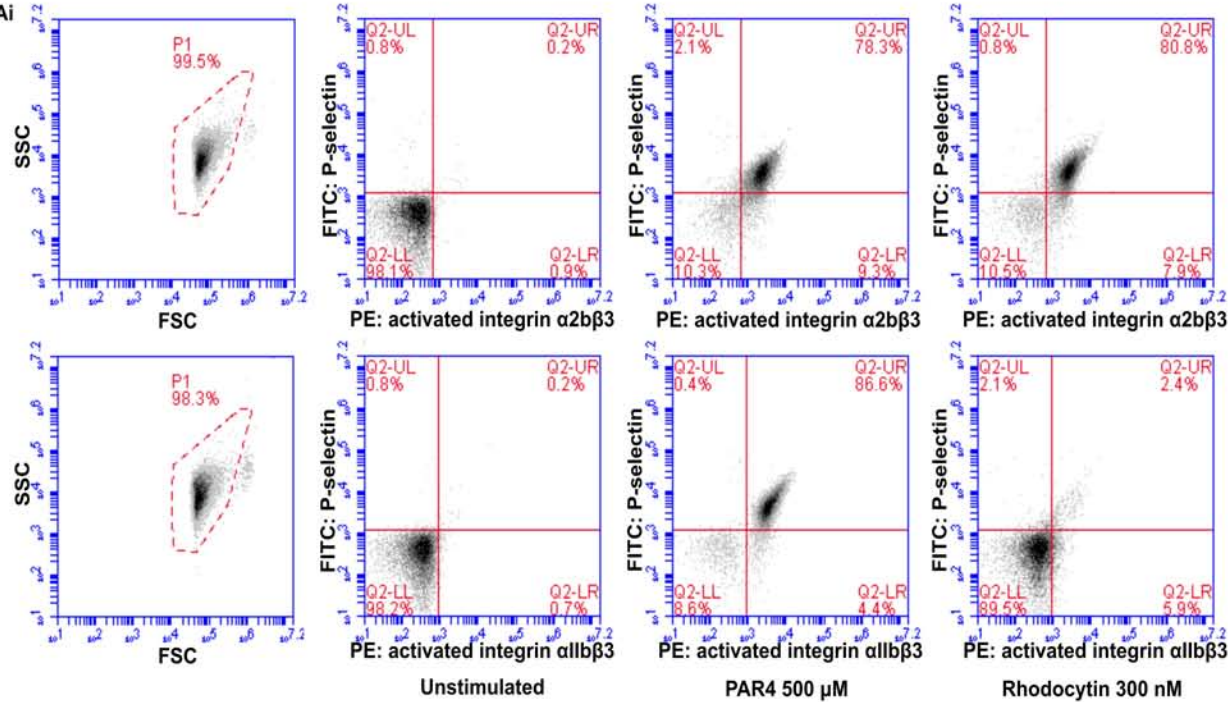
Btk pY223

PLC γ 2 pY753PLC γ 2 pY759PLC γ 2 pY1217

Total Syk

**ii****iii****iv**

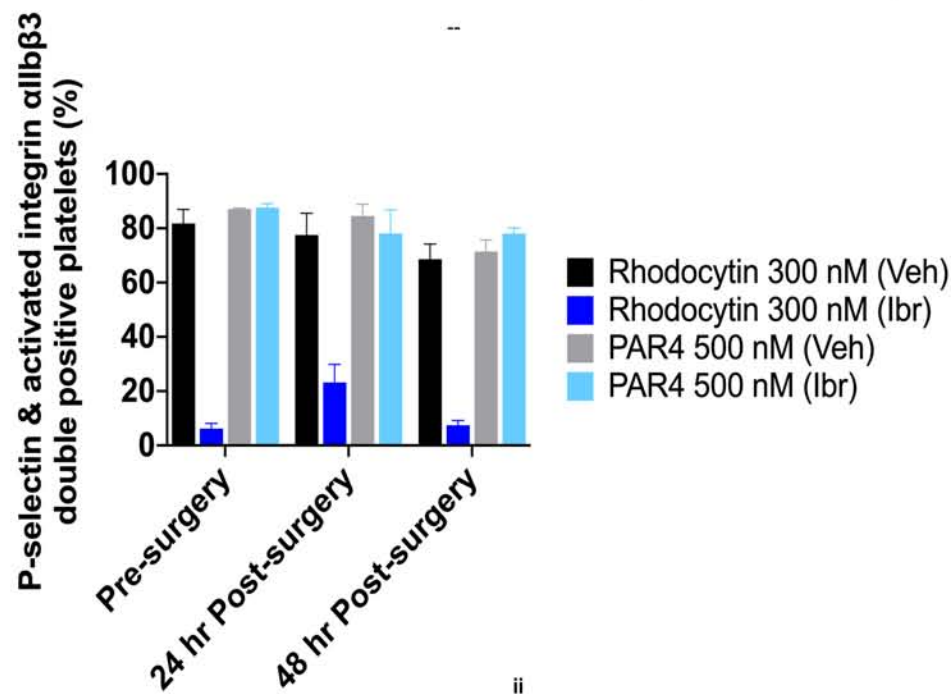
Ai



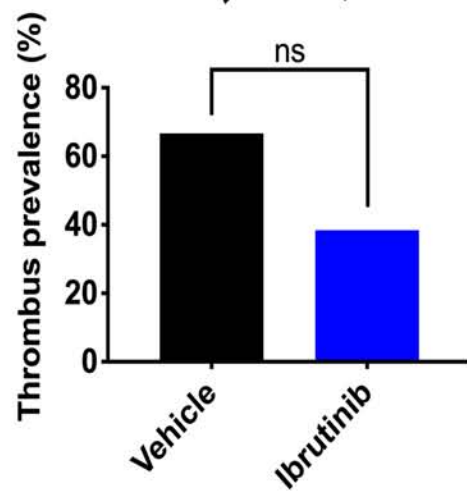
2 hours after pre-surgical dose of vehicle

2 hours after pre-surgical dose of ibrutinib

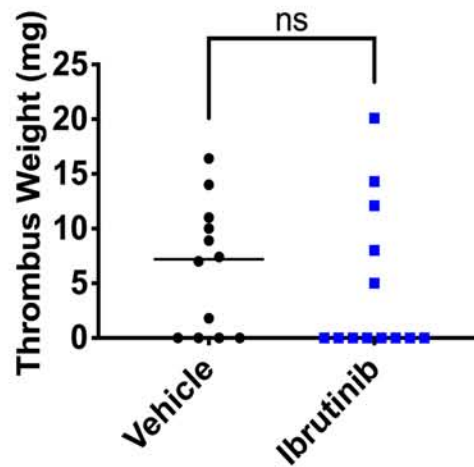
ii



Bi



ii



Supplementary Material

Methods

Reagents

The mouse α -human CLEC-2 antibody AYP1 has been previously described²⁹. α -LAT pAb (06-807) was from Merck Millipore (Burlington, MA). Rhodocytin was isolated according a published protocol³⁰. Human podoplanin-Fc has been previously described³¹. The Btk-deficient DT40 cells, plasmid constructs and rabbit α -Btk antibody were a kind gift from Dr Mike Tomlinson (University of Birmingham, UK). FITC-conjugated anti-mouse P-selectin and PE-conjugated anti-mouse activated α IIb β 3 antibodies were from Emfret (Eibelstadt, Germany). Erythrocyte lysing agent was from Dako (Carpinteria, CA). All other reagents are previously described¹⁶ or are from Sigma-Aldrich (Poole, UK).

Flow cytometry

Heparinised whole mouse blood was obtained by femoral vein sampling and was diluted using phosphate buffered saline (PBS) in the presence or absence of fluorophore conjugated antibody before being stimulated with agonist. This was then incubated with the stated antibodies for 30 minutes at room temperature in the dark. Following this, erythrocytes were lysed and the samples were fixed. Samples were then analysed using an Accuri C6 Flow Cytometer (BD Biosciences, San Jose, CA).

Flow adhesion studies

DiOC₆ labelled whole blood was flowed at 125 s⁻¹ across podoplanin-Fc (100 μ g/ml) coated micro-capillaries within Cellix Vena8 Fluoro+ Biochips (Cellix Limited, Dublin) as previously described³¹.

Imaging

Visualisation of platelet flow adhesion was performed with a 20X objective on a Zeiss Axio Observer 7 microscope (Carl Zeiss AG, Oberkochen, Germany).

Image analysis

Flow adhesion videos were analysed using the KNIME 3.4 analytics platform (KNIME.com AG, Konstanz, Germany)³². Ilastik 1.1.2 machine learning software (University of Heidelberg, Germany) was used to automatically and reproducibly identify platelets³³.

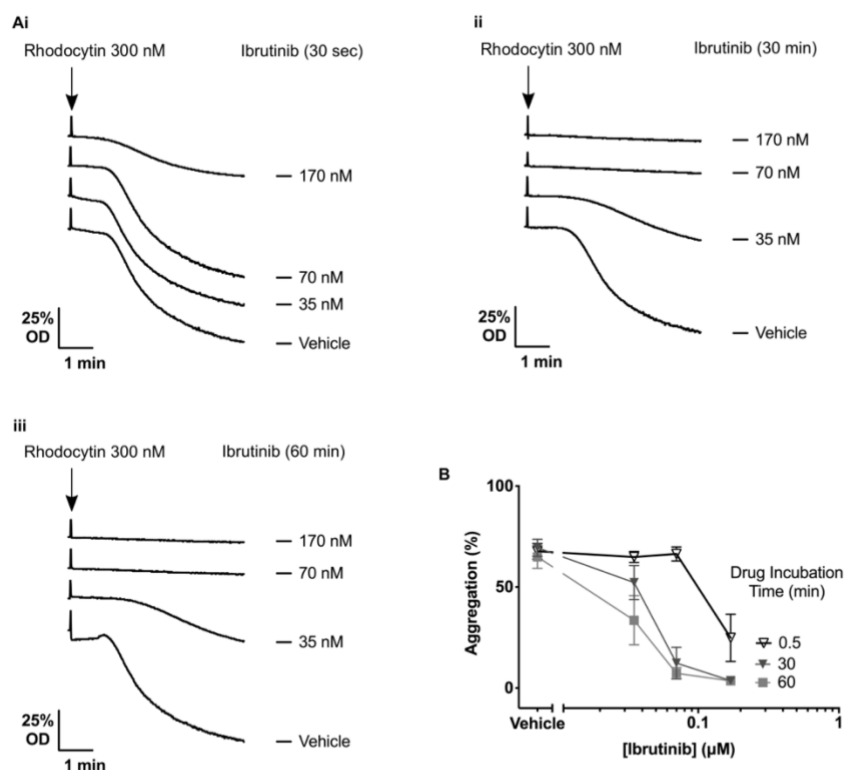
DT40 cell transfection and luciferase assay

DT40 cells were cultured and transfected with 10 μ g of CLEC-2 plasmids as well as NFAT-luciferase and Btk plasmids as previously described¹⁶. Once transfected, cells were stimulated with rhodocytin 50 nM for 6 hours in the presence or absence of ibrutinib (0.5 – 10 μ M), acalabrutinib (0.5 – 10 μ M) or vehicle (DMSO) as stated. Luciferase activity was measured as previously described¹⁶.

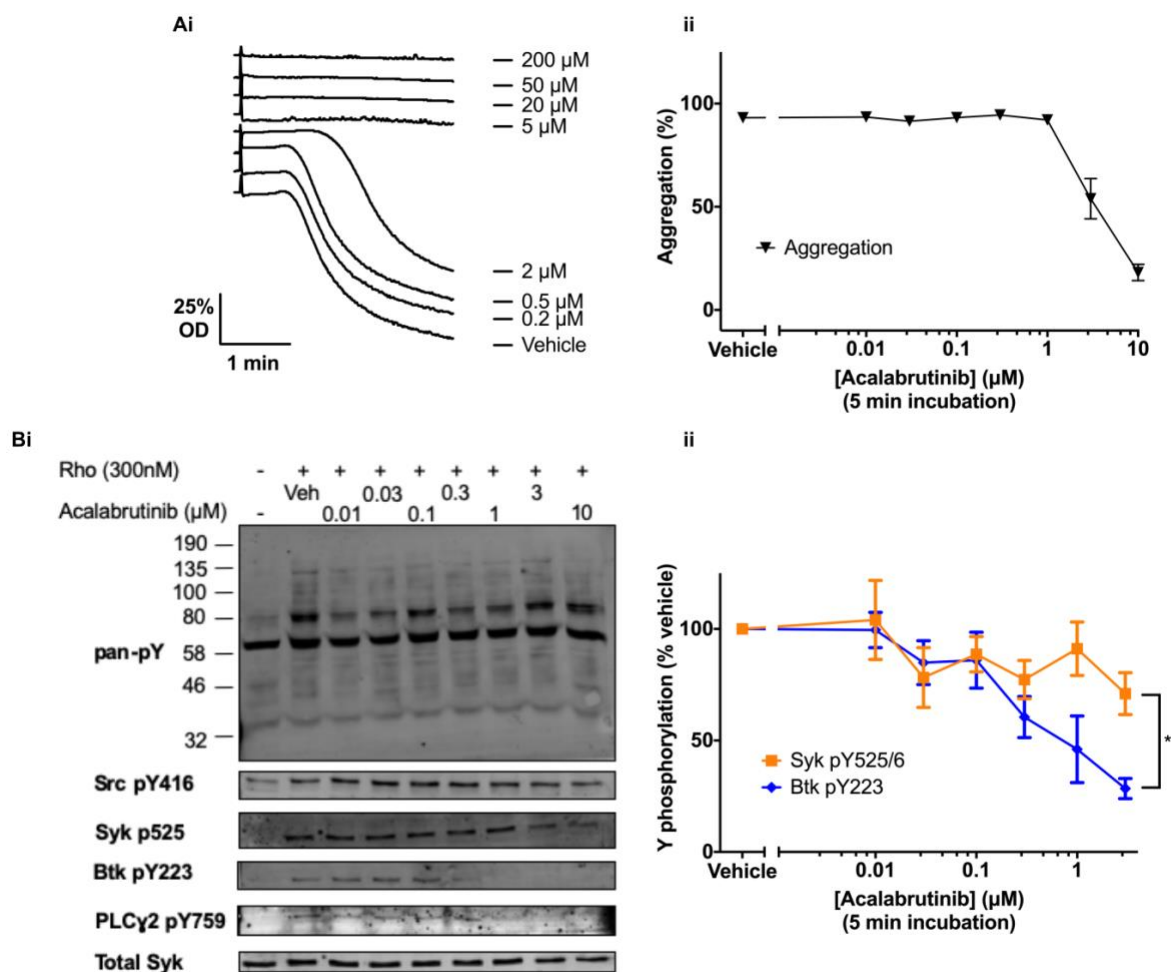
To confirm expression of CLEC-2, cells were pelleted and resuspended in 10 μ g/mL AYP1. Cells were washed and resuspended in AF 488-conjugated goat α -mouse antibody before washing. Cells were resuspended and stained with propidium iodide before flow cytometry analysis using a BD Accuri C6 flow cytometer.

To examine Btk expression, cells were washed in PBS before being pelleted. Pellets were resuspended in 1X RIPA buffer. 6X sample buffer was added to the sample and boiled. Proteins were then separated by SDS -PAGE before western blotting for Btk.

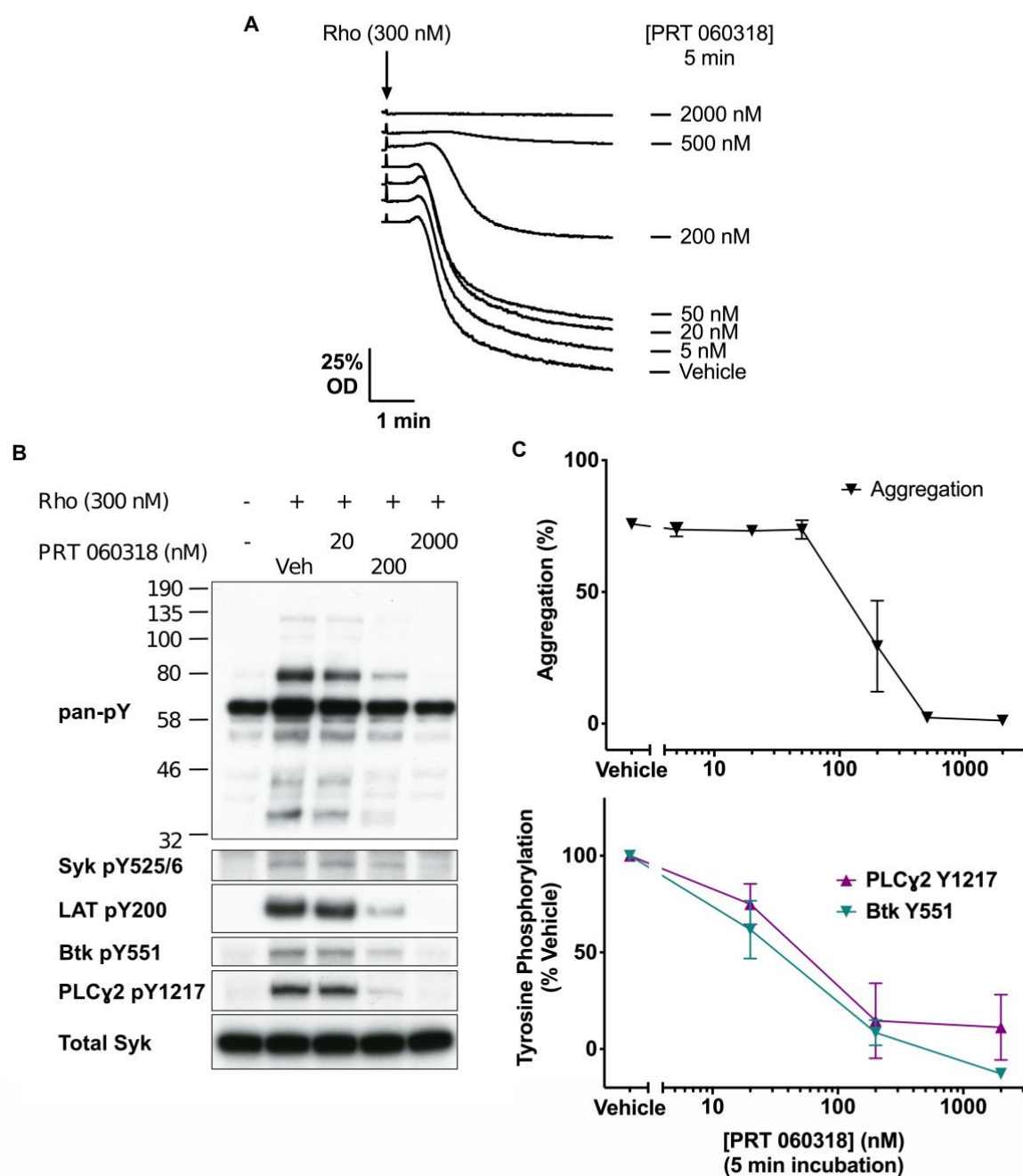
Supplementary Figure 1



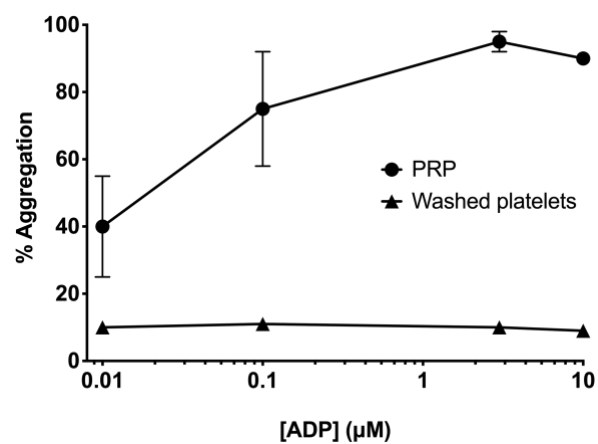
Supplementary Figure 2



Supplementary Figure 3



Supplementary Figure 4



Supplementary Figure 1: Ibrutinib blocks CLEC-2 mediated platelet aggregation in a time-dependent manner. Human healthy donor washed platelets at 4×10^8 /ml were incubated with ibrutinib or vehicle for 30 seconds – 60 minutes before being stimulated with rhodocytin 300 nM for 5 minutes. (A) Representative aggregation traces from one of the five identical experiments. (B) Mean data \pm SEM (n=5) showing the effect of ibrutinib incubation time on CLEC-2-mediated platelet aggregation.

Supplementary Figure 2: Acalabrutinib blocks CLEC-2 mediated platelet aggregation and tyrosine phosphorylation in a dose dependent manner. (A) Healthy donor washed human platelets at 4×10^8 /ml were incubated with acalabrutinib or vehicle (DMSO) for 5 minutes prior to stimulation with 300 nM rhodocytin. LTA measurements were then undertaken for 5 minutes. (i) Representative trace. (ii) Mean data \pm SEM are shown (n=3). (B) Healthy donor washed human platelets at 4×10^8 /ml in the presence of eptifibatide 9 μ M were incubated with acalabrutinib or vehicle (DMSO) for 5 minutes prior to stimulation with 300 nM rhodocytin. Platelets were then lysed with 5X reducing sample buffer 5 minutes after addition of agonist. Whole cell lysates were then separated by SDS-PAGE and western blots were probed for whole cell phosphorylation or kinase phosphorylation with the stated antibodies downstream of the platelet CLEC-2 receptor. (i) Representative blot from 4 identical experiments. (ii) Mean tyrosine levels phosphorylation level \pm SEM of 4 identical experiments for Syk pY525/6 and Btk pY223. Statistical analysis with two-way ANOVA with Sidak's correction for multiple comparisons. *P<0.05.

Supplementary Figure 3: The Syk inhibitor PRT 060318 blocks CLEC-2 mediated platelet aggregation and Btk Y551 phosphorylation. Healthy donor washed human platelets at 4×10^8 /ml were incubated with PRT 060318 or vehicle (DMSO) for 5 minutes prior to stimulation with 300 nM rhodocytin. LTA measurements were then undertaken for 5 minutes. (A) Representative trace and (C) mean data \pm SEM are shown. (B&D) ADP-sensitive healthy donor washed platelets at 4×10^8 /ml were incubated, in the presence of eptifibatide (9 μ M), with PRT 060318 or vehicle for 5 minutes prior to stimulation with 300 nM rhodocytin. Platelets were then lysed with 5X reducing sample buffer 5 minutes after addition of agonist. Whole cell lysates were then separated by SDS-PAGE and western blots were probed for whole cell phosphorylation or kinase phosphorylation with the stated antibodies downstream of the platelet CLEC-2 receptor. (B) Representative blot from 3 identical experiments. (D) Mean tyrosine levels phosphorylation level \pm SEM (n=3) for Btk pY551 and PLC γ 2 pY1217.

Supplementary Figure 4: Washed platelets do not aggregate in response to ADP. PRP and washed platelets (4×10^8 /mL) isolated from healthy donors were stimulated with 0.1 – 10 μ M ADP and LTA measurements were then undertaken for 5 minutes. Dose response curves (n=3) are shown as mean \pm SEM.